



HAL
open science

LEM-domain proteins are lost during human spermiogenesis but BAF and BAF-L persist

Razan A. Elkhatib, Marine Paci, Romain Boissier, Guy Longepied, Yasmina Auguste, Vincent Achard, Patrice Bourgeois, Nicolas Levy, Nicolas Branger, Michael J. Mitchell, et al.

► To cite this version:

Razan A. Elkhatib, Marine Paci, Romain Boissier, Guy Longepied, Yasmina Auguste, et al.. LEM-domain proteins are lost during human spermiogenesis but BAF and BAF-L persist. *Reproduction*, 2017, 154 (4), pp.387-401. 10.1530/REP-17-0358 . hal-01681591

HAL Id: hal-01681591

<https://hal.science/hal-01681591>

Submitted on 16 Apr 2018

HAL is a multi-disciplinary open access archive for the deposit and dissemination of scientific research documents, whether they are published or not. The documents may come from teaching and research institutions in France or abroad, or from public or private research centers.

L'archive ouverte pluridisciplinaire **HAL**, est destinée au dépôt et à la diffusion de documents scientifiques de niveau recherche, publiés ou non, émanant des établissements d'enseignement et de recherche français ou étrangers, des laboratoires publics ou privés.

1

2 **LEM-domain proteins are lost during human spermiogenesis but BAF and**
3 **BAF-L persist**

4

5

6 Razan A. Elkhatib¹, Marine Paci^{1,2}, Romain Boissier³, Guy Longepied¹, Yasmina Auguste
7¹, Vincent Achard^{2,4}, Patrice Bourgeois¹, Nicolas Levy¹, Nicolas Branger³, Michael J
8 Mitchell^{1*} Catherine Metzler-Guillemain^{1,2*}

9

10 *(MJ Mitchell and C Metzler-Guillemain are equal senior authors)

11

12 ¹ Aix Marseille Univ, INSERM, GMGF UMR_S 910, 13385 Marseille, France.

13 ² APHM Hôpital La Conception, Gynépôle, Laboratoire de Biologie de la Reproduction-
14 CECOS, 13385 Marseille cedex 5, France.

15 ³ APHM Hôpital La Conception, Service d'Urologie, 13385 Marseille cedex 5, France

16 ⁴ Aix-Marseille Univ, Laboratoire de Biogénotoxicologie et Mutagenèse Environnementale,
17 EA 1784 – Fédération de Recherche CNRS n°3098 Ecosystèmes Continentaux et Risques
18 Environnementaux, 13385 Marseille cedex 5, France.

19

20

21

22

23 **Short title:**

24 LEM-domain and BAF proteins in spermiogenesis

25

26 Abstract - 248 words

27 During spermiogenesis the spermatid nucleus is elongated, and dramatically reduced in size
28 with protamines replacing histones to produce a highly compacted chromatin. After
29 fertilisation, this process is reversed in the oocyte to form the male pronucleus. Emerging
30 evidence, including the coordinated loss of the nuclear lamina (NL) and the histones, supports
31 the involvement of the NL in spermatid nuclear remodelling, but how the NL links to the
32 chromatin is not known. In somatic cells, interactions between the NL and the chromatin have
33 been demonstrated: LEM-domain proteins and LBR interact with the NL and, respectively,
34 the chromatin proteins BAF and HP1. We therefore sought to characterise the lamina-
35 chromatin interface during spermiogenesis, by investigating the localisation of six LEM-
36 domain proteins, two BAF proteins, and LBR, in human spermatids and spermatozoa. Using
37 RT-PCR, IF and Western blotting, we show that six of the proteins tested are present in
38 spermatids: LEMD1, LEMD2 (a short isoform), ANKLE2, LAP2 β , BAF and BAF-L, and
39 three absent: Emerin, LBR and LEMD3. The full-length LEMD2 isoform, required for
40 nuclear integrity in somatic cells, is absent. In spermatids, no protein localised to the nuclear
41 periphery, but five were nucleoplasmic, receding towards the posterior nuclear pole as
42 spermatids matured. Our study therefore establishes that the lamina-chromatin interface in
43 human spermatids is radically distinct from that defined in somatic cells. In ejaculated
44 spermatozoa, we detected only BAF and BAF-L, suggesting that they might contribute to the
45 shaping of the spermatozoon nucleus and, after fertilisation, its transition to the male
46 pronucleus.

47

48

49

50 Key words: LEM-domain/ BAF/ spermiogenesis/ human/ Nuclear Lamina

51

52 **Introduction**

53 Spermiogenesis is the post-meiotic phase of spermatogenesis when haploid round spermatids
54 undergo a dramatic transformation into mature elongated spermatozoa. This involves nuclear
55 remodelling, chromatin condensation, replacement of nuclear histones with protamines and
56 formation of an acrosomal cap and a flagellum at opposite poles of the spermatid nucleus.
57 Although the precise mechanisms are not yet fully elucidated, it is certain that these processes
58 are in part coordinated by interactions between the nuclear envelope (NE) and specialised
59 cytoskeletal elements of the spermatid, the acroplaxome and the manchette (Kierszenbaum
60 and Tres, 2004).

61 The NE of eukaryotic cells is composed of the two nuclear membranes, the nuclear
62 lamina (NL) and the nuclear pore complexes (NPC) that create channels between the
63 nucleoplasm and the cytoplasm. The outer nuclear membrane (ONM) is continuous with the
64 endoplasmic reticulum (ER), while the inner nuclear membrane (INM) is lined on its
65 nucleoplasmic face by the NL, a peripheral network of type V intermediate filaments, called
66 lamins, involved in chromatin organization, cell cycle regulation, DNA replication, cell
67 differentiation, gene expression and apoptosis (Burke and Stewart, 2013). During
68 spermiogenesis in human and mouse the NL is composed exclusively of B-type lamins, and
69 retreats from the anterior to the posterior pole as the acrosome spreads and the histones are
70 removed from the chromatin (Alzheimer *et al.* 2004; De Vries *et al.* 2012; Elkhatib *et al.*
71 2015).

72 The NL is known to connect to the cytoskeleton through the interaction of SUN and
73 KASH proteins that span the nuclear membranes. In spermatids, the proteins SUN3, SUN4

74 and SUN5 have a localisation coincident with the lamins (Göb *et al.* 2010; Calvi *et al.* 2015;
75 Yassine *et al.* 2015). In mice lacking SUN4, spermatids do not elongate, and spermatozoa
76 have round heads (globozoospermia-like) (Calvi *et al.* 2015; Pasch *et al.* 2015). Biallelic loss-
77 of-function mutations in *SUN5* have been found in men with acephalic spermatozoa syndrome
78 (Zhu *et al.* 2016; Elkhatib *et al.* 2017). True globozoospermia is observed in mice and men
79 lacking DPY19L2, an INM protein localised under the acrosome (Harbuz *et al.* 2011;
80 Koscinski *et al.* 2011; Pierre *et al.* 2012). In mice lacking DPY19L2, the acrosome detaches,
81 elongation does not occur and lamins remain throughout the nuclear periphery of spermatozoa
82 (Pierre *et al.* 2012; Yassine *et al.* 2015). There is therefore good evidence that the NL has
83 central roles in shaping functional spermatozoa.

84 In contrast, little is known about how the NL interacts with the chromatin during
85 spermiogenesis, despite the identification of proteins that form links between the NL and the
86 chromatin in somatic cells: Lamin B Receptor (LBR), members of the LEM-domain (the
87 Lamina-associated polypeptide 2, Emerin, MAN1 domain) protein family and Barrier-to-
88 Autointegration Factor (BAF) (Goldman *et al.* 2002; Gruenbaum *et al.* 2005; Schirmer and
89 Foisner, 2007). LBR was the first integral membrane protein of the INM to be identified
90 (Worman *et al.* 1988). LBR binds lamin B1 and links the lamina to the chromatin through an
91 interaction with the HP1-type heterochromatin proteins (Ye and Worman, 1994; Ye *et al.*
92 1997). Human LEM-domain proteins are a heterogeneous family of mainly nuclear proteins
93 that share a conserved ~40 amino acid domain, the LEM-domain, named after three LEM-
94 domain proteins shown to bind BAF: LAP2, EMERIN and MAN1 (aka LEMD3) (Furukawa,
95 1999; Cai *et al.* 2001; Lee *et al.* 2001; Shumaker *et al.* 2001; Mansharamani and Wilson,
96 2005). In addition to the founding proteins, four further human LEM-domain encoding genes
97 have been described: LEMD1, with testis-predominant transcription (Yuki *et al.* 2004),
98 LEMD2, required for nuclear integrity (Brachner *et al.* 2005), ANKLE2, a regulator of BAF

99 phosphorylation with a role in post-mitotic nuclear envelop formation (Lee and Wilson,
100 2004; Asencio *et al.* 2012) and ANKLE1, an endonuclease possibly involved in DNA repair
101 (Brachner *et al.* 2012).

102 BAF, a conserved metazoan chromatin protein (Lee and Craigie, 1998) plays a key
103 role in post-mitotic nuclear assembly (Margalit *et al.* 2007). It forms homodimers that can
104 simultaneously bind dsDNA molecules and a LEM-domain (Shumaker *et al.* 2001; Segura-
105 Totten *et al.* 2002). BAF is expressed widely, but has a paralogue, barrier-to-autointegration
106 factor-like (BAF-L) that is expressed predominately in testis and pancreas (Tift *et al.* 2006;
107 Margalit *et al.* 2007). Human BAF-L and BAF share 40% amino acid identity. BAF-L was
108 described as specific to mammals (Margalit *et al.* 2007), but recent additions to the databases
109 indicate that BAF-L is specific to vertebrates. Unlike BAF, BAF-L does not bind DNA. BAF-
110 L does form heterodimers with BAF, and it may thus modulate BAF chromatin functions in
111 testis and pancreas (Tift *et al.* 2006).

112 Except for LBR and LAP2 isoforms, none of these proteins has been studied during
113 mammalian spermiogenesis. LBR has been localised to the nuclear periphery of elongating
114 spermatids in the rat, where a role in chromatin remodelling during spermiogenesis has been
115 proposed based on the detection, *in vitro*, of an interaction with Protamine 1 (Mylonis *et al.*
116 2004). The LAP2 isoforms have also been studied in the rat, where LAP2 β predominates in
117 spermatids, but only LAP2 α persists in mature spermatozoa (Alsheimer *et al.* 1998). Thus as a
118 first step towards defining how the NL interfaces with the chromatin during spermiogenesis,
119 we have characterised the expression of LBR, BAF, BAF-L and six LEM-domain proteins in
120 human spermatids and spermatozoa.

121 **Material & Methods**

122 ***Patients***

123 Sperm samples were obtained from fourteen normospermic men who consulted at our
124 reproduction centre or gamete bank (CECOS - Centre d'Etude et de Conservation des Oeufs
125 et du Sperme) in Marseilles: ten men consulted for couple infertility (9 primary and 1
126 secondary infertility), four men were fertile sperm donors (Table 1).

127 Testicular samples came from four patients with brain death, who were 21, 31, 50 and 65
128 years old. Testicular samples were obtained within a protocol, approved by the French
129 Research Minister, for the collection of human tissue for use in research. We declared our
130 protocol through the Biomedicine Agency in January 2013. Testes were recovered during
131 multi-organ retrieval for transplantation while the patient was under extracorporeal circulation
132 and respiratory assistance. All patients had normal spermatogenesis based on histology
133 analysis and retrieval of numerous spermatozoa after testis dilaceration and one of the four
134 patients had children (T011400063, T011400051, T011400071 and T011500055).

135

136 ***Semen and testicular samples***

137 Semen was collected via masturbation after a period of sexual abstinence of 2-6 days. After
138 30 minutes of liquefaction, semen analysis was performed according to the WHO criteria
139 (WHO Association, 2009), and according to the French David classification for the
140 morphology analysis (Auger *et al.* 2016). Sperm was diluted in cryoprotectant medium
141 (Spermfreeze; JCD, La Mulatière, France) and transferred into straws (Cryo Bio System,
142 Saint Ouen sur Iton, France). Straws were then suspended in vapour-phase nitrogen before
143 being stored in liquid nitrogen until use. All patients gave an informed consent for the
144 conservation of the remnant sperm in the Germetheque biobank and their use in studies on
145 human fertility in accordance with the Helsinki Declaration of 1975 on human
146 experimentation. The Germetheque Scientific Committee approved the present study design.

147 All sperm samples came from patients with normal sperm parameters according to WHO
148 criteria (Table 1).

149 Testicular cells fixed in 4% paraformaldehyde in phosphate buffered saline (PBS) before
150 freezing from the four patients (T011400063, T011400051, T011400071 and T011500055)
151 were used.

152

153 *Spermatozoa RNA extraction*

154 Following storage in liquid nitrogen, sample straws were thawed and the sperm was washed
155 twice in 2 ml of PBS, and then suspended in round cell lysis buffer (0.1% SDS, 0.5% Triton
156 X-100 in RNase free H₂O). RNA was extracted with 1ml of Tripure (Roche) and precipitated
157 with 20 µg of glycogen as carrier. RNAs were treated with 10 units of DNase I, at room
158 temperature 10 minutes, in 1X reverse transcriptase buffer with 10 mM DTT and 20 units of
159 Protector RNase inhibitor (Roche).

160

161 *RT-PCR and quality control of spermatozoa RNA extracts*

162 Before reverse transcription, RNA was purified on chromaspin 100 (Clontech) or Nucleospin
163 RNA XS columns (Macherey Nagel). Concentration was determined using a nanodrop ND-
164 1000 spectrophotometer (NanoDrop Technologies, Wilmington, DE, USA). RNAs (400 ng)
165 were reverse transcribed in a 20 µl reaction with random nanomers (75 pmoles) and Expand
166 Reverse Transcriptase (Roche). The resulting cDNA was diluted to 40 µl with water and 1 µl
167 used in subsequent PCR amplification with Q5 High-Fidelity DNA Polymerase (New
168 England Biolabs).

169 Control PCRs were carried out with standard Taq polymerase. We checked for the presence
170 of spermatid RNA derived cDNAs by amplifying the protamine 1 transcript with primers
171 o1680/o1681 annealed at 60 °C. We checked for the lack of contaminating round cell RNA

172 by Polymerase chain reactions using a triplex reaction with primers for *PTPRC* (*CD45*), *KIT*
173 and *CDH1* which are positive markers for leukocytes, early testicular germ cells and epithelial
174 cells respectively (Lambard *et al.* 2004). Triplex primers and concentrations: *PTPRC* (310 bp)
175 - o4609/o4610, 300 nM; c-Kit (237 bp) - o4611/o4612, 500 nM; *CDH1* 136 bp -
176 o4613/o4614, 500 nM. PCR programme 94 °C 2 min, 94 °C 30 s, 60 °C 40 s, 72°C 20 s 40
177 cycles, 72 °C 5 min.

178 LEM-domain proteins transcripts were amplified with Q5 Taq polymerase (New England
179 Biolabs) using the PCR conditions described in the product information. The primer pairs and
180 their annealing temperature for each transcript are as follows: LEMD1: o4426/o4427 – 66 °C,
181 LEMD2-3': o4092/o4093 – 68°C, LEMD2-5':o4965/o4966 – 69°C, LEMD3-3':
182 o5023/o4491– 66 °C, LEMD3-5': o5024/o5026 – 67°C, EMERIN-3': o5097/o5098 – 69°C,
183 EMERIN-5': o5095/o5096 – 67°C, ANKLE1-3': o5027/o4493 – 67°C, ANKLE1-5':
184 o5028/o5029 – 72°C, ANKLE2-3': o4495/o4496 – 68°C, ANKLE2-5': o5111/o5112 – 70°C,
185 ANKLE2_Δ1-64: o4527/o4528 – 71°C, LAP2-5': o5101/o5103 – 68°C LAP2α 3':
186 o4087/o4088 – 64°C, LAP2β 3': o5099/o5100 – 68°C, LAP2β-5': o4087/o4090 – 64°C,
187 BAF: o4094/o4095 – 69°C, BAF-L: o4096/o4097 – 69°C, LBR-3': o4667/o4668 – 60°C,
188 LBR-5': o4669/o4671 – 64°C, musLEMD1: o4435/o4434 – 67°C, musBAF-L: o4522/o4523
189 – 67°C, musHMBS: o2216/o2217 – 67°C, PRM1: o1680/o1681 – 60°C. PRM1, a spermatid-
190 specific spermatozoa-retained transcript was included as a positive control for spermatozoa
191 RNA. The Q5 GC-enhancer additive was used for all PCRs except for LBR. (Sequences of
192 primers are provided in supplementary Table S1).

193 **Constructs to express tagged proteins**

194 To express fusion proteins tagged with either 3xc-Myc (Myc) or 3xFlag (Flag), the coding
195 region for each protein was amplified by PCR from human testis cDNA, using specific
196 primers with restriction sites added at the 5' end. The PCR products were digested at these

197 added sites and ligated to a vector cut with the same enzymes. The vectors were modified
198 pcDNA3.1 vector (Life Technologies) carrying either an N-terminal tag between *NheI* and
199 *HindIII* sites or a C-terminal tag between *BamHI* and *XbaI* sites. The primers used are shown
200 in Table S1. Flag-ANKLE2, primers: o4573/o4710, cloning sites: *KpnI* and *BamHI*. Flag-
201 ANKLE2-Δ1-64, primers: o4542/o4710, cloning sites: *KpnI* and *BamHI*. LEMD2-myc and
202 LEMD2_Δ115-259-myc, primer: o5322/o5323, cloning sites: *HindIII* and *KpnI*. BAF-Flag,
203 primers: o4388/o4399, cloning sites: *KpnI* and *BamHI*. Flag-BAF-L, primers: o5186/o4663,
204 cloning sites: *KpnI* and *XhoI*. myc-LEMD1, primers: o4661/o4659, cloning sites *KpnI* and
205 *XhoI*. myc-Emerin, primers: o4579/o4580, cloning sites: *BamHI* and *XhoI*. myc-LAP2β,
206 primers: o5022/o4615, cloning sites: *BamHI* and *XhoI*. All constructs used were confirmed to
207 have the expected sequence by determining the sequence of the full insert and tag.

208 ***Cell culture and transfection***

209 HeLa cells were cultured according to standard procedures.
210 Cells were transfected in two-well Lab-tek chambers using jetPRIME® short-DNA
211 transfection protocol (Polyplus-transfection) and 500 ng of plasmid DNA according to the
212 manufacturer's instructions. The medium was replaced after 4 hours of incubation with the
213 transfection mix.

214 ***Immunocytochemistry***

215 Immunocytochemistry was performed on spread spermatozoa and/or testicular germ cells.
216 Thawed spermatozoa were washed two times in PBS, fixed in 2% formaldehyde in PBS for
217 10 min, washed twice in PBS and spread onto polylysine-coated slides by Cytospin
218 (Shandon). Testicular cells were fixed with 2% formaldehyde in PBS for 10 min after
219 disaggregation of testis fragments, washed in PBS and pellets frozen. Testicular cell pellets
220 were thawed and spread onto polylysine slides by Cytospin (Shandon) as previously described
221 (Metzler-Guillemain and Guichaoua, 2000). Slides were fixed 5 minutes in 4% formaldehyde

222 in PBS, rinsed in PBS and permeabilized using 0.1%, 0.3% or 0.5% Triton X-100, 3% normal
223 goat serum in PBS for 30 min. Slides were blocked with 1% BSA, 7% normal goat serum in
224 PBS for 30 min. They were then incubated for 30 min with lectins (Lectin PNA Alexa Fluor
225 594 conjugates, L-21409 Molecular Probes) at a dilution of 1:600 in PBS to mark the
226 acrosome. After washes in PBS under gentle agitation, slides were incubated one to two hours
227 in a moist chamber at 37°C with primary antibodies after several washes in PBS, detection
228 was performed using Alexa fluor secondary antibodies (Invitrogen) at dilutions recommended
229 by manufacturers for 45 min at 37°C. Slides were then rinsed twice in PBS and mounted with
230 25 to 75 ng/ml DAPI in Vectashield mounting medium for microscope analysis. Negative
231 controls without the primary antibody gave no signal for any of the secondary antibodies
232 used. The slides were analyzed using the Zeiss ApoTome.2 microscope (Zeiss, Oberkochen,
233 Germany) equipped with an AxioCam MRm camera. Images were captured and merged with
234 the ZEN software, and were treated using ImageJ software. Phase contrast overlay of
235 ANKLE2 immunofluorescent labelling shows that cell morphology is preserved by this
236 protocol (Fig. S1).

237 **Antibodies**

238 The affinity of antibodies for their target was validated for IF analysis using HeLa cells
239 transfected with a construct overexpressing a tagged version of the target protein, except for
240 those against LBR and LEMD3, already shown by the supplier to label the nuclear periphery
241 in HeLa cells (Fig. S2). All antibodies used were monoclonal or immunogen affinity-purified
242 polyclonal and gave the expected labelling pattern in somatic cells in disaggregated testes:
243 nuclear periphery for LEMD2, LEMD3, Emerin, LAP2 β , LBR and BAF; endoplasmic
244 reticulum for ANKLE2; faint or no labelling for LEMD1 and BAF-L (only spermatid nuclei
245 labelled). We provide representative images of single large fields obtained for each antibody

246 to show the labelling of germ cells and somatic cells observed together in disaggregated testes
247 (Fig. S3).

248 The antibodies used were rabbit anti-LEMD1 (IF dilution: 1/100, SAB3500644
249 Sigma), rabbit anti-LEMD2 specific N-terminus (IF dilution: 1/100, HPA017340 Sigma),
250 rabbit anti-LEMD2 specific C-terminus (IF dilution: 1/50, ab89866 Abcam), mouse anti-
251 LEMD3 (IF dilution: 1/50, ab123973 Abcam), mouse anti-EMERIN (IF dilution: 1/100,
252 NCL-EMERIN Leica), mouse anti-EMERIN (IF dilution: 1/100, Sigma AMAb90560), rabbit
253 anti-ANKLE2 (IF dilution: 1/100, Asencio *et al.* 2012), rabbit anti-LAP2 beta (IF dilution:
254 1/50, HPA008150 sigma), rabbit anti-BAF (IF dilution: 1/600 ab129184 Abcam), rabbit anti-
255 BAF-L (IF dilution: 1/100, HPA042635 Sigma), rabbit anti-BAF-L (IF dilution: 1/200,
256 ab122950 Abcam), rabbit anti LBR (IF dilution: 1/500, ab32535 Abcam), mouse anti-FLAG
257 (IF dilution: 1/100, F1804 Sigma), mouse anti-c-MYC (IF dilution: 1/100, sc40 Santa Cruz) ,
258 rabbit anti- α tubulin (WB dilution: 1/1000, ab15246 Abcam) and anti-GRP94 (IF dilution:
259 1/400, ab210960) (Table S2).

260 The immunogen peptide used for pre-absorption of anti-BAF (within amino acids 1-
261 45) was custom synthesised (Proteogenix, France). The immunogen peptide for BAF-L (aa
262 12-252) was expressed as a fusion protein with the chitin binding protein in *E. coli* and
263 purified on a chitin column, following the protocol of the Impact Kit (New England Biolabs),
264 except that the BAF-L fusion protein was eluted with 8M Urea and then dialysed against PBS.
265 The BAF-L coding region was amplified with primers o5350/o5351 and cloned between the
266 *NdeI* and *XhoI* sites of the pMXB10 vector (New England Biolabs). Pre-absorption
267 protocol***

268 **Protein extraction and western blot analysis**

269 Protein was prepared from 12×10^6 spermatozoa which were separated from round cells as for
270 RNA extraction, and then lysed on ice for 30 min in 100 μ l of 0.5% SDS, 50 mM Tris.HCl

271 pH8.0, 5 mM EDTA, 50 mM DTT, 2x complete proteinase inhibitor cocktail (Roche),
272 followed by 30 s of sonication at high setting in a Bioruptor Standard (Diagenode). The
273 effectiveness of the round cell lysis is illustrated by the absence of a signal for Emerin,
274 despite the strong signal in whole testis (Fig. S4). Emerin is strongly detected in testicular
275 somatic cells, but we did not detect it by IF in spermatids or spermatozoa. For testis lysates,
276 60 mg of tissue was dissociated in 300 ml of lysis buffer (1M Tris.HCl pH7.5, 5M NaCl, 0.1
277 mM EGTA, 10% Triton) using ceramic beads in a Magnalyser (Roche), followed by 30 min
278 on ice and 3x 30 s of sonication at high setting in a Bioruptor Standard (Diagenode). For
279 migration, lysate from approximately 2 million spermatozoa or 40 µg of testis protein was
280 mixed with 2x Laemmli sample loading buffer loading buffer (Sigma Aldrich) with 5% β-
281 mercaptoethanol, heated to 95 °C for 5 minutes and subjected to SDS-PAGE. Proteins were
282 blotted on to nitrocellulose with a pore size of 0.45 µm (Emerin) or 0.2 µm (BAF, BAF-L).

283

284 **Results**

285 **Spermatid transcript analysis using spermatozoa RNA**

286 To characterise gene expression of NL-associated proteins (LBR, LEM-domain proteins, BAF
287 and BAF-L) during human spermiogenesis, we first used RT-PCR to detect the 5' and 3' end
288 of the coding region of transcripts, in spermatozoa RNA from five normospermic men: two
289 fertile men and three men from infertile couples. RT-PCR detected transcripts for Emerin,
290 LEMD1, LEMD2, ANKLE2, LAP2α, LAP2β and BAF-L in all tested RNA samples (Fig. 1),
291 but in the case of LEMD2 only the 3' end of the coding region was detected, indicating that
292 the only transcript present for LEMD2 in spermatids lacks a part of the 5' coding region
293 present in the widely expressed form. No transcripts were detected for LBR, LEMD3 or
294 ANKLE1 in any sample (Fig. 1).

295 BAF transcripts were detected in one RNA sample R010900491 but not in the other
296 four, suggesting that they are normally absent from spermatozoa (Fig. 1). BAF is encoded by
297 the *BANFI* gene, and has five retroposed homologues in the genome. We therefore
298 investigated the nature of the *BANFI* cDNA product amplified from R010900491 by
299 sequencing and revealed it to be identical to the *BANFI* locus, excluding the possibility that it
300 was derived from one of the *BANFI* retroposons. In addition, we did not amplify the same
301 cDNA product from the genomic DNA of R010900491, excluding the possibility that
302 R010900491 carries a recently integrated *BANFI* retroposon with 100% nucleotide identity to
303 *BANFI*. The individual in whose sperm sample we detected BAF transcripts is normospermic
304 and his sperm does not have an exceptional morphology or motility profile. He is nevertheless
305 in an infertile couple, and it will now be important to define the relationship between BAF
306 transcript retention in spermatozoa and gamete quality. We conclude that the *BANFI*
307 transcript can persist in spermatozoa in a minority of cases, but whether this is related to
308 increased RNA stability, epigenetic variation or the quality of spermatogenesis remains to be
309 elucidated.

310

311 **BAF-L and LEMD1 transcripts coincide with spermatids in immature mouse testis.**

312 Having shown that transcripts for the testis-predominant genes *BANF2* and *LEMD1*
313 were present in human spermatids, we next investigated transcription from these genes during
314 the first wave of post-natal spermatogenesis in the mouse. We found that transcripts for both
315 genes were detected only at later steps (after 20 dpp) when spermatids first appear in the testis
316 (Fig. 2). We conclude that BAF-L and *LEMD1* transcripts predominate in spermatids in
317 mouse and human.

318

319 **Alternative transcript for *ANKLE2* in spermatids**

320 For ANKLE2, we detected a transcript (ANKLE2_Δ 1-64) corresponding to several
321 testis ESTs with an alternative first exon situated within the first intron (*e.g.* HY008086) (Fig.
322 3A). We amplified ANKLE2_Δ 1-64 from all five spermatozoa RNA samples (Fig. 3B), and
323 from total RNA of testis and brain, but not small intestine, skeletal muscle, prostate or thymus
324 (Fig. 3C). In the mouse, no EST corresponding to this transcript has been described, and we
325 did not detect a homologous transcript from the mouse *Ankle2* gene by RT-PCR with primers
326 from candidate alternative first exons in intron 1 defined by splice donor site prediction (data
327 not shown). We amplified as a single amplicon and then sequenced the full coding region of
328 the ANKLE2_Δ 1-64 transcript from human testis RNA and deposited its sequence in
329 Genbank (accession KY056762). The ANKLE2_Δ 1-64 transcript encodes an ANKLE2
330 isoform lacking the N-terminal 64 amino acids that encode the transmembrane domain of the
331 full-length isoform which are replaced by the short peptide of five amino acids ¹MWRSE⁵.

332

333 ANKLE2_Δ 1-64 does not localise to the endoplasmic reticulum in HeLa cells

334 The full-length ANKLE2 protein has been localised to the nuclear periphery and endoplasmic
335 reticulum (ER) (Asencio *et al.* 2012). To test the intracellular localization of ANKLE2_Δ 1-
336 64, we transfected HeLa cells with plasmids designed to express N-terminus Flag-tagged
337 versions of the full-length ANKLE2 and ANKLE2_Δ 1-64, under control of the CMV
338 promoter. Following transfection, Flag-ANKLE2 had a granular aspect throughout the
339 cytoplasm that we show co-localises with the ER marker GRP94, consistent with the ER
340 localisation described previously for ANKLE2 (Asencio *et al.* 2012). In contrast Flag-
341 ANKLE2_Δ 1-64 was more homogeneously distributed throughout the cytoplasm, and did
342 not coincide with GRP94 (Fig. 4A). We conclude that the N-terminal 64 aa of ANKLE2,
343 which contain the TM, are required to locate ANKLE2 to the ER in HeLa cells.

344

345 ANKLE2 localises to the ER in round spermatids

346 We investigated the localisation of ANKLE2 during spermiogenesis by
347 immunofluorescent analysis of testicular germ cells from four men and ejaculated
348 spermatozoa from three men. An ANKLE2 signal was detected throughout human
349 spermiogenesis, in the cytoplasm of round spermatids, elongating spermatids and testicular
350 spermatozoa***, but was not visible in ejaculated spermatozoa. In round spermatids, it
351 presented as a granular cytoplasmic signal, consistent with the known localisation of
352 ANKLE2 to the ER (Fig. 4B). We confirmed ER localisation for ANKLE2 in round
353 spermatids, by showing that the signal co-localises with the ER-lumen protein GRP94 (Fig.
354 4C). In elongating spermatids, however, there was no longer a perfect coincidence of GRP94
355 and ANKLE2 signals, a possible reflection of the distinct localisation of ANKLE2 (ER
356 cytoplasmic surface) and GRP94 (ER lumen). We saw no evidence of the more diffuse
357 cytoplasmic staining that might correspond to the ANKLE2_Δ1-64 isoform that lacks the
358 domain necessary for ER localisation (Fig. 4B, C).

359

360 LEMD2 transcript in spermatids encodes a short isoform

361 To identify the LEMD2 transcript present in human spermatids, we initially screened testis
362 and spermatozoa RNA with RT-PCR assays based on ESTs in the databases that lack the first
363 coding exon of LEMD2 (DC315891, DC367547, BI755923, DB028937 and DC389488), but
364 no product was amplified from testis T011400071 or spermatozoa RNA (data not shown). We
365 next amplified the entire LEMD2 coding region from testis RNA and observed a doublet, a
366 band of the expected size (1.5 kb) and a smaller band (1.1 kb) (Fig. 5A). We cloned and
367 sequenced these fragments. The larger fragment contained the full coding region as predicted
368 while the smaller fragment contained two cDNAs created by alternative splicing from a
369 cryptic splice donor site immediately following codon 114 (c.346) in exon 1, to either exon 2

370 (frameshift) or to exon 3 (non-frameshift) (Fig. 5A). Using specific RT-PCR assays for each
371 transcript we found that both alternatives are present in spermatozoa RNA (shown for the
372 non-frameshift transcript in Fig. 5B). We conclude that the only protein-coding transcript
373 from *LEMD2* in spermatids encodes a short version of LEMD2 that we have termed
374 *LEMD2_Δ115-259* since it lacks amino acids 115-259 of the full-length protein. The cryptic
375 splice site in exon 1 that allows the production of the alternative transcripts is not present in
376 mouse and we were unable to detect corresponding transcripts in the mouse (data not shown).
377 We PCR amplified and cloned the coding region of the *LEMD2_Δ115-259* transcript as a
378 single amplicon from testis cDNA, sequenced it and deposited it in Genbank (accession
379 KY056761).

380

381 ***LEMD2_Δ115-259* is not directed to nuclear periphery and does not destabilise NE**

382 It has been concluded that LEMD2 is important for nuclear integrity, since its depletion from
383 somatic cells leads to altered nuclear morphology (Ulbert *et al.* 2006), similar to that induced
384 by ectopic expression of the spermatid-specific lamin B3 (Schütz *et al.* 2005; Elkhatib *et al.*
385 2015). We therefore investigated the possibility that *LEMD2_Δ115-259* has a role in
386 destabilising the NE to facilitate nuclear remodelling in spermatids. To do this we expressed
387 both isoforms with a C-terminal Flag-tag in HeLa cells. We observed that while the full-
388 length isoform was directed to the nuclear periphery as expected, *LEMD2_Δ115-259* was not,
389 and was visible in the perinuclear region of the cytoplasm. *LEMD2_Δ115-259* did not induce
390 any nuclear deformation (Fig. 5C). Taken together with previous work (Brachner *et al.* 2005)
391 showing that LEMD2 lacking amino acids 130-203 is directed to the nuclear periphery, our
392 results show that at least part of a domain necessary for the import of LEMD2 from the
393 cytoplasm to the nuclear periphery, must be located within aa 115-130 and aa 203-259. In
394 addition, our IF analysis of transfected cells shows that the anti-LEMD2 antibody

395 HPA017340, whose immunogen (aa 243-362) overlaps with amino acids 115-259 of LEMD2
396 is essentially specific for the full-length LEMD2 isoform, and does not detect LEMD2_Δ115-
397 259 (Fig. 5C). The epitopes detected with high affinity by HPA017340 must therefore all
398 overlap with aa 243-259 of LEMD2.

399

400 **Nuclear LEM-domain proteins and LBR not at nuclear periphery in human spermatids**

401 In order to explore the nature of the interface between the NL and the chromatin during
402 human spermiogenesis, we performed IF analysis of testicular germ cells from four men with
403 antibodies against six LEM-domain proteins, the two BAF proteins and LBR (antibody
404 descriptions - Table S2). We detected signals on spermatids for LEMD1, LEMD2, ANKLE2,
405 LAP2β, BAF and BAF-L (Fig. 6, Fig. S3 and Table 2), but no signal was observed on
406 spermatids with antibodies against Emerin, LBR or LEMD3, despite strong labelling of the
407 nuclear periphery in somatic cells on the same slide (Fig. S5, S4).

408 For Emerin, we had amplified a transcript from spermatozoa RNA by RT-PCR, and it
409 was therefore unexpected that Emerin was not detected in spermatids. We therefore tested two
410 different anti-Emerin antibodies that labelled the nuclear periphery in somatic cells (Fig. S6).
411 Neither labelled any spermatids or spermatozoa (Leica-Emerin-Ncl and AMAb90560) (Fig.
412 S6). Moreover, in Human Protein Atlas, a further two antibodies, HPA000609 and
413 CAB001545, do not label spermatids. Thus although we have shown that the Emerin
414 transcript is present in spermatids, we conclude that it is not translated and that the Emerin
415 protein is not present in spermatids or spermatozoa.

416 Using antibodies directed against LEMD1 we observed a nucleoplasmic signal in
417 round spermatids, except in the area covered by the acrosome. As spermatid maturation
418 progressed, the fluorescence became limited progressively to the posterior pole of the nuclei,

419 where it remained visible in late elongated spermatids. LEMD1 was not detected, however, on
420 testicular spermatozoa or on ejaculated spermatozoa (Fig. 6).

421 For LEMD2, our RT-PCR analyses suggested that in spermatids LEMD2 was only
422 present as an isoform lacking amino acids 115-259. We therefore analysed testicular germ
423 cells with two antibodies, anti-LEMD2_243-362 (Sigma HPA017340) that detects the full-
424 length LEMD2 isoform but not LEMD2_Δ115-259 (Fig. 5C and S3), and anti-LEMD2_Cter
425 that detects both isoforms (Fig. S2). Despite strong labelling of the nuclear periphery in
426 somatic cells of disaggregated testis with both antibodies, only anti-LEMD2_Cter labelled the
427 nuclei of spermatids, confirming that in spermatids, LEMD2 is present only as the short
428 isoform LEMD2_Δ115-259 (Fig. 6 and Fig. S3). Anti-LEMD2_Cter gave a punctate labelling
429 throughout the spermatid nucleoplasm, indicating that LEMD2_Δ115-259 does not localise to
430 the nuclear periphery in spermatids (Fig. 5C).

431 For LAP2β, labelling is nuclear, and predominates at the nuclear periphery in the
432 earliest round, spermatids but the signal shifts to the nucleoplasm at later steps and is not
433 detected in elongating spermatids (Fig. 6). In the rat, the nucleoplasm and NE labelling in
434 round spermatids were previously demonstrated with an antibody that detected all LAP2
435 isoforms (Alzheimer *et al.* 1998). The anti-BAF-L antibody gave a granular signal
436 concentrated over the nucleoplasm of round spermatids, with fainter fluorescence in the
437 cytoplasm. Labelling was concentrated at the nuclear periphery in elongating spermatids, but
438 was excluded from under the acrosome (Fig. 6). In testicular and ejaculated spermatozoa
439 BAF-L labelling was visible at the posterior pole of the nucleus (Fig. 7A).

440 Although no BAF transcript was detected in spermatozoa RNA from four of five men
441 tested, the anti-BAF antibody (ab129184) labelled the nuclei of spermatids (Fig. 6). We
442 observed a nucleoplasmic localization of BAF in 10% - 55% of round spermatids, 2% - 9% of
443 elongated spermatids, and 1% - 10% of testicular spermatozoa, where BAF was located at the

444 posterior pole of the nucleus (Fig. 6 and Fig. S7A and S5B). BAF signal was observed in
445 ejaculated spermatozoa at the posterior nuclear pole in all 3 patients tested with a mean of 30
446 % of spermatozoa labelled (Fig. 7A). These contradictory results for the expression of the
447 BAF protein and its transcript imply either that the BAF spermatid transcript is a remnant
448 from spermatocytes (BAF protein labelling is seen throughout the spermatocyte nucleus - Fig.
449 S7C), or that *de novo* BAF transcripts are produced in spermatids but are not retained in
450 spermatozoa.

451

452 **BAF and BAF-L are present in human ejaculated spermatozoa**

453 Our IF analyses of human spermatids indicate that most of the proteins tested as potential
454 links between the NL and the chromatin are lost during the round spermatid steps and do not
455 persist in spermatozoa. The only exceptions were with the antibodies against BAF and BAF-L
456 that labelled the posterior nuclear pole of testicular and ejaculated spermatozoa. These signals
457 were absent when we pre-absorbed the antibodies with their respective immunising peptide,
458 indicating that they were specific for BAF and BAF-L (Fig. 7A). To further verify that this
459 signal was due to the presence of BAF and BAF-L, we performed Western blot analysis of
460 lysates of purified spermatozoa with the same antibodies (Fig. 7B). The anti-BAF and anti-
461 BAF-L antibodies detected a strong band of the expected size, approximately 10 kDa, in
462 protein lysates from spermatozoa. Anti-BAF detected a strong band of the same size in testis
463 lysates, but in the case of BAF-L the band was barely detectable in whole testis, suggesting
464 that it is expressed in spermatids at a low level and becomes concentrated in the spermatozoa
465 fraction (Fig. 7B). We conclude that BAF and BAF-L proteins are present in spermatids
466 throughout human spermiogenesis and are retained in ejaculated spermatozoa.

467

468 **Discussion**

469 Known somatic lamina-chromatin interface absent from all but earliest spermatids

470 Here we present an overview of how LEM-domain proteins, BAF proteins and LBR,
471 many known to be involved in linking the NL to the chromatin in somatic cells, are organised
472 in human spermatids and spermatozoa. For most of the proteins, except LBR and LAP2 β , this
473 is the first study of these proteins during mammalian spermiogenesis. We have studied
474 ANKLE1 and LAP2 α expression only at the transcript level.

475 Based on our observations, a general theme emerges that during most of
476 spermiogenesis the lamina-chromatin interface, as defined in somatic cells, does not exist, and
477 the three LEM-domain proteins that we did detect, LEMD1, LEMD2_ Δ 115-259 and LAP2 β ,
478 do not localise to the nuclear envelope in most round spermatids, but to the nucleoplasm. This
479 can readily be explained for LEMD2_ Δ 115-259 based on our HeLa transfection experiments
480 showing that LEMD2_ Δ 115-259 lacks the domains required for NE localisation, consistent
481 with the mapping of these domains to aa 74-130 and aa 203-378 (Brachner *et al.* 2005). It is
482 more difficult to explain the nucleoplasmic localisation of LEMD1 and LAP2 β . Both contain
483 a transmembrane domain (TM), which has been shown to be necessary for the efficient
484 localisation of LAP2 β to the NE (Furukawa *et al.* 1995). LAP2 β is found at the inner nuclear
485 membrane in somatic cells (Foisner and Gerace, 1993) (Fig. S3) and tagged-LEM1
486 transfected into HeLa cells localises, like Emerin (Tsuchiya *et al.* 1999), to a perinuclear
487 cytoplasmic structure and the nuclear envelope (Fig. S2). Indeed, LAP2 β is peripheral in the
488 earliest round spermatids, but becomes exclusively nucleoplasmic at all later steps (Fig. 6).
489 We suggest that proteins required for the direction of LEMD1 and LAP2 β to the NE in
490 somatic cells are unavailable in spermatids or that spermatid-specific proteins direct them to
491 the nucleoplasm.

492 LAP2 β is known to localise to the NE in part by interacting with lamin B1 (Furukawa
493 *et al.* 1998), which is present at the INM in human spermatids (Elkhatib *et al.* 2015). It is

494 therefore possible that changes in the nuclear lamina block the access of LAP2 β to lamin B1.
495 It is unlikely that loss of LAP2 β from the NE in spermatids is a direct consequence of lamin
496 B3 recruitment or LEMD2 absence because it has been shown that overexpression of lamin
497 B3 or knockdown of LEMD2 in HeLa cells does not affect the localisation of LAP2 β to the
498 NE (Schütz *et al.* 2005; Ulbert *et al.* 2006). Nevertheless, the displacement of LAP2 β from
499 the nuclear periphery could have a functional significance during spermiogenesis, since BAF-
500 L and LEMD1, which are predominantly expressed in human and mouse spermatids (Fig. 2),
501 are also nucleoplasmic in round spermatids (Fig. 6; Fig. S3).

502 The absence of the known somatic lamina-chromatin interface from most spermatids
503 is probably related to the unique extreme chromatin remodelling that occurs during
504 spermiogenesis. It is interesting that the somatic lamina-chromatin interface is no longer
505 required in round spermatids even though there is still a high transcriptional activity to
506 produce the proteins that will allow the round spermatid to become a spermatozoon. Indeed
507 the priority in spermatids may be to detach the chromatin from the lamina to increase
508 accessibility for histone-protamine exchange, since the lamina itself gradually disappears
509 from the nuclear periphery in synchrony with the spread of protamine-packed chromatin
510 (Alzheimer *et al.* 2004; De Vries *et al.* 2012; Elkhatib *et al.* 2015). We do not know whether a
511 specific structure continues to link the histone-packed chromatin to the lamina in spermatids,
512 or whether the lamina becomes completely detached from the chromatin early during
513 spermiogenesis. One way of exploring the former possibility would be to try to identify
514 partners of lamin B1 or lamin B3 in purified round spermatids.

515

516 **LBR is not detected in human spermatids**

517 We did not detect expression of LBR in spermatids at either the RNA or the protein level. In
518 the mouse, LBR has been localised to the nuclear periphery in elongating spermatids, and

519 based on an interaction in transfected cells with protamine 1, it has been suggested that LBR
520 plays a role in the replacement of histones by protamines during spermiogenesis (Mylonis *et*
521 *al.* 2004). Our finding is supported by results with anti-LBR antibody HPA049840 (Human
522 Protein Atlas) that labels the nuclear periphery of only the spermatogonia in the seminiferous
523 tubule. This discrepancy with the mouse may indicate that LBR is expressed differently
524 between rodents and human, or it might arise from a lack of antibody specificity in the mouse
525 study, where the antibody against mouse LBR was raised against the N-terminal amino acids
526 1-201 that includes a conserved highly immunogenic stretch ($^{78}\text{SRSRSRSRSRSRSP}^{91}$) that
527 contains peptides found in more than a hundred different mouse proteins. In contrast, the LBR
528 epitopes detected by the antibody ab32535 (aa 1-60) that we used here, and HPA049840 (aa
529 1-71) that is presented in Human Protein Atlas do not overlap with $^{78}\text{SRSRSRSRSRSRSP}^{91}$.
530 Whatever the explanation for this discrepancy, our data together with those in Human Protein
531 Atlas provide strong evidence that LBR is not present in human spermatids, and is therefore
532 not involved in the deposition of protamine 1 onto the chromatin during human
533 spermiogenesis.

534

535 **Increasing flexibility of the spermatid NL**

536 In mouse and human, the lamin B2 isoform, lamin B3, is recruited to the NE during
537 spermiogenesis and has been demonstrated to deform the NE when expressed in cultured cells
538 (Schütz *et al.* 2005; Elkhatib *et al.* 2015). This has been interpreted to indicate that the
539 flexibility of the spermatid NE is increased to facilitate the remodelling of the nucleus into an
540 elongated form. We have shown, however, that neither LEMD2_Δ115-259 nor ANKLE2_Δ1-
541 64 share the ability of lamin B3 to deform the NE when transfected into HeLa cells. We have
542 also found that orthologous transcripts for LEMD2_Δ115-259 or ANKLE2_Δ1-64 are not
543 expressed in the mouse (data not shown). We conclude that the ANKLE2_Δ1-64 and

544 LEMD2_Δ115-259 transcripts are either biological artefacts or primate-specific measures to
545 regulate ANKLE2 and LEMD2 expression. It has however been shown that the reduction of
546 LEMD2 level in HeLa cells (Ulbert *et al.* 2006) causes the same type of nuclear deformations
547 as the ectopic expression of lamin B3. Thus the absence of the full-length LEMD2 isoform
548 from the spermatid nucleus, with lamin B3 expression, could be part of the same strategy to
549 produce a flexible NE. We conclude that it is more likely the absence of the full-length
550 conserved LEMD2 isoform, and not the presence of the LEMD2_Δ115-259 isoform, that has
551 functional significance for the shaping of the spermatozoon nucleus.

552

553

554 **BAF and BAF-L may regulate condensation of the paternal chromatin**

555 Our finding that both BAF and BAF-L are present in spermatozoa is an exciting one. Indeed,
556 on Western blot analysis, the signal obtained for each protein is at least as strong in
557 spermatozoa as in whole testis, implying that both are abundant in spermatozoa. This is very
558 obvious for BAF-L where we detected a very weak signal in whole testis (Fig. 7B). This
559 implies that the retention of BAF and BAF-L in spermatozoa may be functionally important.
560 BAF and BAF-L both form homodimers, but are able to form heterodimers *in vitro* and on co-
561 transfection into cultured cell lines (Tiffit *et al.* 2006). BAF can bind DNA and LAP2β
562 simultaneously, but BAF-L cannot bind DNA or LAP2β on its own (Tiffit *et al.* 2006).
563 Nevertheless BAF-BAF-L heterodimers are able to bind DNA and LAP2β (Tiffit *et al.* 2006).
564 Furthermore we have shown that ANKLE2, necessary for the recruitment of BAF to the
565 chromatin at mitotic exit (Asencio *et al.* 2012), is present on the ER in round spermatids. It is
566 therefore of critical significance that both BAF and BAF-L proteins are present in spermatids
567 and spermatozoa, since it opens up the possibility that, through its interaction with BAF,
568 BAF-L could be a component of the sperm chromatin.

569 The specific role of BAF-L during spermiogenesis is unclear, but the formation of
570 BAF-BAF-L heterodimers might serve to prevent BAF homodimer formation on the
571 nucleohistone chromatin of round spermatids. BAF homodimers are able to cross-link two
572 double stranded DNA molecules, form dodecamer complexes with dsDNA, and induce
573 condensation of the chromatin (Zheng *et al.* 2000; Skoko *et al.* 2009). In contrast, BAF-BAF-
574 L heterodimers can only bind to a single DNA molecule and so could promote a more open
575 chromatin that facilitates the massive histone-protamine exchanges that occur during
576 spermiogenesis and during the formation of the male pronucleus in the oocyte cytoplasm. In
577 support of this hypothesis, the concentration of BAF has been shown to be critical for correct
578 chromatin decondensation of sperm chromatin in *Xenopus* egg extracts, with as little as a
579 20% increase in BAF concentration inducing excessive chromatin condensation and
580 preventing NE assembly (Segura-Totten *et al.* 2002).

581

582 **BAF-L may regulate timing of NE formation on paternal chromatin in oocytes**

583 In mouse and *Xenopus* oocytes, the formation of a sealed nuclear membrane can occur
584 around the paternal chromatin artificially depleted for nucleosomes, but in the absence of
585 nucleosomes, nuclear pore complexes are not recruited, preventing nuclear import notably of
586 NL components, and a failure of nuclear expansion and zygotic development (Inoue and
587 Zhang, 2014; Zierhut *et al.* 2014). A mechanism must therefore exist that ensures delay of
588 nuclear membrane assembly on the paternal chromatin until the histones have been integrated.
589 In somatic cells, BAF recruitment to the surface of the chromosomes at mitotic exit is an early
590 and essential step in the reassembly of the NE (Haraguchi *et al.* 2008). Furthermore BAF can
591 behave like a DNA-sensor and binds rapidly to histone-free dsDNA transferred into the
592 cytoplasm of cultured cells, promoting assembly of NE-like membranes (Kobayashi *et al.*

593 2015). Thus, another possible role for BAF-L in the oocyte could be to delay the onset of
594 BAF-dependent assembly of the NE until after nucleosome incorporation.

595

596 **Conclusion and Perspectives**

597 Our study reveals that, except for LAP2b in the earliest round spermatids, none of the
598 components of the NL-chromatin interface defined in somatic cells is present at the nuclear
599 periphery of germ cells during human spermiogenesis, and the definition of the NL-chromatin
600 interface in spermatids, if it exists, now requires the identification of proteins that interact
601 with lamin B1 and lamin B3 in spermatids.

602 An important finding of our study is that BAF and BAF-L are present in ejaculated
603 human spermatozoa, where they could be chromatin components with roles in the formation
604 of the spermatozoon nucleus and its transformation into the male pronucleus. Our study
605 therefore opens new perspectives for the study of paternal chromatin remodelling, during
606 spermiogenesis and immediately after fertilisation, that we will now explore through the study
607 of mice inactivated for BAF-L. We predict that, given BAF's central role in mitosis, and the
608 severe somatic phenotype associated with loss of BAF function (Puente *et al.* 2011), it will
609 be extremely unlikely to find BAF mutations causal of isolated male infertility in human.
610 Mutations in BAF-L however, with its spermatid-predominant expression, could cause
611 isolated male infertility and might be found by targeting infertile men whose spermatozoa
612 retain high levels of histones or fail to achieve a functional pronucleus following *in vitro*
613 fertilisation. We will use the mouse model to better predict the spermatogenic phenotype that
614 might be associated with loss of BAF-L function in men. Studying the roles of BAF and
615 BAF-L in the context of male fertility should provide fresh insights into the relationship
616 between chromatin remodelling and the quality of the sperm nucleus.

617

618 Author's contribution

619 RAE performed most of the experimental work, and was involved in the manuscript writing.
620 MP and YA were involved in immunofluorescence techniques. CMG, RB, PB, VA and NB
621 played a role in the patient recruitment. GL organised and supervised cell transfection and
622 RT-PCR experiments. MJM performed western blot experiments; CMG was particularly
623 involved in the study conception and the manuscript writing with MJM, RAE and NL. CMG
624 and MJM took direct responsibility for the manuscript. All authors contributed to the writing
625 and revision of the manuscript.

626

627 Funding

628 This work was supported by grants from the Agence de la biomédecine, AOR “AMP,
629 diagnostic prenatal et diagnostic génétique” 2013, Inserm and Aix-Marseille Université. The
630 Germetheque biobank was supported by grants from the ANR (Agence Nationale de la
631 Recherche), the Agence de la biomédecine, the Centre Hospitalier Universitaire of Toulouse
632 and APHM (Assistance Publique Hôpitaux de Marseille). RAE was funded by the Islamic
633 Development Bank and the Lebanese Association for Scientific Research (LASeR).

634

635

636 Conflict of interest

637 All authors declare no conflict of interest

638

639 Acknowledgements

640 We are grateful to the patients who gave their informed consent to the use of their samples for
641 research. We thank doctor J. C. Colavolpe and the “Coordination Hospitalière de Prélèvement

642 d'Organes et de Tissus" team for their help collecting human testis samples, C. Metton and
643 M.J. Fays-Bernardin for technical assistance and Germetheque support.

644

645 **References**

646 **Alsheimer M, Fecher E & Benavente R** 1998 Nuclear envelope remodelling during rat
647 spermiogenesis: distribution and expression pattern of LAP2/thymopoietins. *Journal of Cell*
648 *Science* **111** 2227–2234.

649 **Alsheimer M, Liebe B, Sewell L, Stewart CL, Scherthan H & Benavente R** 2004
650 Disruption of spermatogenesis in mice lacking A-type lamins. *Journal of Cell Science* **117**
651 1173–1178.

652 **Asencio C, Davidson IF, Santarella-Mellwig R, Ly-Hartig TBN, Mall M, Wallenfang**
653 **MR, Mattaj IW & Gorjánácz M** 2012 Coordination of kinase and phosphatase activities by
654 Lem4 enables nuclear envelope reassembly during mitosis. *Cell* **150** 122–135.

655 **Auger J, Jouannet P & Eustache F** 2016 Another look at human sperm morphology.
656 *Human Reproduction (Oxford, England)* **31** 10–23.

657 **Brachner A, Reipert S, Foisner R & Gotzmann J** 2005 LEM2 is a novel MAN1-related
658 inner nuclear membrane protein associated with A-type lamins. *Journal of Cell Science* **118**
659 5797–5810.

660 **Brachner, A, J Braun, M Ghodgaonkar, D Castor, L Zlopasa, V Ehrlich, J Jiricny, J**
661 **Gotzmann, S Knasmuller & R Foisner** 2012 The endonuclease Ankle1 requires its LEM
662 and GIY-YIG motifs for DNA cleavage in vivo. *J Cell Sci* **125** 1048-1057.

663 **Burke B & Stewart CL** 2013 The nuclear lamins: flexibility in function. *Nature Reviews.*
664 *Molecular Cell Biology* **14** 13–24.

665 **Cai M, Huang Y, Ghirlando R, Wilson KL, Craigie R & Clore GM** 2001 Solution
666 structure of the constant region of nuclear envelope protein LAP2 reveals two LEM-domain

LEM-domain proteins during human spermiogenesis

12/06/2017

28

- 667 structures: one binds BAF and the other binds DNA. *The EMBO Journal* **20** 4399–4407.
- 668 **Calvi A, Wong ASW, Wright G, Wong ESM, Loo TH, Stewart CL & Burke B** 2015
- 669 SUN4 is essential for nuclear remodeling during mammalian spermiogenesis. *Developmental*
- 670 *Biology* **407** 321–330.
- 671 **De Vries M, Ramos L, Housein Z & De Boer P** 2012 Chromatin remodelling initiation
- 672 during human spermiogenesis. *Biology Open* **1** 446–457.
- 673 **Elkhatib R, Longepied G, Paci M, Achard V, Grillo J-M, Levy N, Mitchell MJ &**
- 674 **Metzler-Guillemain C** 2015 Nuclear envelope remodelling during human spermiogenesis
- 675 involves somatic B-type lamins and a spermatid-specific B3 lamin isoform. *Molecular*
- 676 *Human Reproduction* **21** 225–236.
- 677 **Elkhatib, RA, M Paci, G Longepied, J Saias-Magnan, B Courbiere, MR Guichaoua, N**
- 678 **Levy, C Metzler-Guillemain & MJ Mitchell** 2017 Homozygous deletion of SUN5 in three
- 679 men with decapitated spermatozoa. *Human molecular genetics* doi: 10.1093/hmg/ddx200.
- 680 [Epub ahead of print].
- 681 **Foisner R & Gerace L** 1993 Integral membrane proteins of the nuclear envelope interact
- 682 with lamins and chromosomes, and binding is modulated by mitotic phosphorylation. *Cell* **73**
- 683 1267–1279.
- 684 **Furukawa K** 1999 LAP2 binding protein 1 (L2BP1/BAF) is a candidate mediator of LAP2-
- 685 chromatin interaction. *Journal of Cell Science* **112** 2485–2492.
- 686 **Furukawa K, Panté N, Aebi U & Gerace L** 1995 Cloning of a cDNA for lamina-associated
- 687 polypeptide 2 (LAP2) and identification of regions that specify targeting to the nuclear
- 688 envelope. *The EMBO Journal* **14** 1626–1636.
- 689 **Furukawa K, Fritze CE & Gerace L** 1998 The major nuclear envelope targeting domain of
- 690 LAP2 coincides with its lamin binding region but is distinct from its chromatin interaction
- 691 domain. *The Journal of Biological Chemistry* **273** 4213–4219.

LEM-domain proteins during human spermiogenesis

12/06/2017

29

- 692 **Göb E, Schmitt J, Benavente R & Alsheimer M** 2010 Mammalian sperm head formation
693 involves different polarization of two novel LINC complexes. *PloS One* **5** e12072.
- 694 **Goldman RD, Gruenbaum Y, Moir RD, Shumaker DK & Spann TP** 2002 Nuclear
695 lamins: building blocks of nuclear architecture. *Genes & Development* **16** 533–547.
- 696 **Gruenbaum Y, Margalit A, Goldman RD, Shumaker DK & Wilson KL** 2005 The nuclear
697 lamina comes of age. *Nature Reviews. Molecular Cell Biology* **6** 21–31.
- 698 **Haraguchi T, Kojidani T, Koujin T, Shimi T, Osakada H, Mori C, Yamamoto A &**
699 **Hiraoka Y** 2008 Live cell imaging and electron microscopy reveal dynamic processes of
700 BAF-directed nuclear envelope assembly. *Journal of Cell Science* **121** 2540–2554.
- 701 **Harbuz R, Zouari R, Pierre V, Ben Khelifa M, Kharouf M, Coutton C, Merdassi G,**
702 **Abada F, Escoffier J, Nikas Y et al.** 2011 A recurrent deletion of DPY19L2 causes
703 infertility in man by blocking sperm head elongation and acrosome formation. *American*
704 *Journal of Human Genetics* **88** 351–361.
- 705 **Inoue A & Zhang Y** 2014 Nucleosome assembly is required for nuclear pore complex
706 assembly in mouse zygotes. *Nature Structural & Molecular Biology* **21** 609–616.
- 707 **Kierszenbaum AL & Tres LL** 2004 The acrosome-acroplaxome-manchette complex and the
708 shaping of the spermatid head. *Archives of Histology and Cytology* **67** 271–284.
- 709 **Kobayashi S, Koujin T, Kojidani T, Osakada H, Mori C, Hiraoka Y & Haraguchi T**
710 2015 BAF is a cytosolic DNA sensor that leads to exogenous DNA avoiding autophagy.
711 *Proceedings of the National Academy of Sciences of the United States of America* **112** 7027–
712 7032.
- 713 **Koscinski I, Elinati E, Fossard C, Redin C, Muller J, Velez de la Calle J, Schmitt F, Ben**
714 **Khelifa M, Ray PF, Kilani Z et al.** 2011 DPY19L2 deletion as a major cause of
715 globozoospermia. *American Journal of Human Genetics* **88** 344–350.
- 716 **Lambard S, Galeraud-Denis I, Saunders PTK & Carreau S** 2004 Human immature germ

LEM-domain proteins during human spermiogenesis

12/06/2017

30

- 717 cells and ejaculated spermatozoa contain aromatase and oestrogen receptors. *Journal of*
718 *Molecular Endocrinology* **32** 279–289.
- 719 **Lee MS & Craigie R** 1998 A previously unidentified host protein protects retroviral DNA
720 from autointegration. *Proceedings of the National Academy of Sciences of the United States of*
721 *America* **95** 1528–1533.
- 722 **Lee KK & Wilson KL** 2004 All in the family: evidence for four new LEM-domain proteins
723 Lem2 (NET-25), Lem3, Lem4 and Lem5 in the human genome. *Symposia of the Society for*
724 *Experimental Biology* 329–339.
- 725 **Lee KK, Haraguchi T, Lee RS, Koujin T, Hiraoka Y & Wilson KL** 2001 Distinct
726 functional domains in emerin bind lamin A and DNA-bridging protein BAF. *Journal of Cell*
727 *Science* **114** 4567–4573.
- 728 **Mansharamani M & Wilson KL** 2005 Direct binding of nuclear membrane protein MAN1
729 to emerin in vitro and two modes of binding to barrier-to-autointegration factor. *The Journal*
730 *of Biological Chemistry* **280** 13863–13870.
- 731 **Margalit A, Brachner A, Gotzmann J, Foisner R & Gruenbaum Y** 2007 Barrier-to-
732 autointegration factor--a BAFfling little protein. *Trends in Cell Biology* **17** 202–208.
- 733 **Metzler-Guillemain C & Guichaoua MR** 2000 A simple and reliable method for meiotic
734 studies on testicular samples used for intracytoplasmic sperm injection. *Fertility and Sterility*
735 **74** 916–919.
- 736 **Mylonis I, Drosou V, Brancorsini S, Nikolakaki E, Sassone-Corsi P & Giannakouros T**
737 2004 Temporal association of protamine 1 with the inner nuclear membrane protein lamin B
738 receptor during spermiogenesis. *The Journal of Biological Chemistry* **279** 11626–11631.
- 739 **Pasch E, Link J, Beck C, Scheuerle S & Alsheimer M** 2015 The LINC complex component
740 Sun4 plays a crucial role in sperm head formation and fertility. *Biology Open* **4** 1792–1802.
- 741 **Pierre V, Martinez G, Coutton C, Delaroche J, Yassine S, Novella C, Pernet-Gallay K,**

LEM-domain proteins during human spermiogenesis

12/06/2017

31

- 742 **Hennebicq S, Ray PF & Arnoult C** 2012 Absence of Dpy19l2, a new inner nuclear
743 membrane protein, causes globozoospermia in mice by preventing the anchoring of the
744 acrosome to the nucleus. *Development (Cambridge, England)* **139** 2955–2965.
- 745 **Puente, XS, V Quesada, FG Osorio, R Cabanillas, J Cadinanos, JM Fraile, GR Ordonez,**
746 **DA Puente, A Gutierrez-Fernandez, M Fanjul-Fernandez et al.** 2011 Exome sequencing
747 and functional analysis identifies BANF1 mutation as the cause of a hereditary progeroid
748 syndrome. *American journal of human genetics* **88** 650–656.
- 749 **Schirmer EC & Foisner R** 2007 Proteins that associate with lamins: many faces, many
750 functions. *Experimental Cell Research* **313** 2167–2179.
- 751 **Schütz W, Benavente R & Alsheimer M** 2005 Dynamic properties of germ line-specific
752 lamin B3: the role of the shortened rod domain. *European Journal of Cell Biology* **84** 649–
753 662.
- 754 **Segura-Totten M, Kowalski AK, Craigie R & Wilson KL** 2002 Barrier-to-autointegration
755 factor: major roles in chromatin decondensation and nuclear assembly. *The Journal of Cell*
756 *Biology* **158** 475–485.
- 757 **Shumaker DK, Lee KK, Tanhehco YC, Craigie R & Wilson KL** 2001 LAP2 binds to
758 BAF.DNA complexes: requirement for the LEM domain and modulation by variable regions.
759 *The EMBO Journal* **20** 1754–1764.
- 760 **Skoko D, Li M, Huang Y, Mizuuchi M, Cai M, Bradley CM, Pease PJ, Xiao B, Marko**
761 **JF, Craigie R et al.** 2009 Barrier-to-autointegration factor (BAF) condenses DNA by
762 looping. *Proceedings of the National Academy of Sciences of the United States of America*
763 **106** 16610–16615.
- 764 **Tiftt KE, Segura-Totten M, Lee KK & Wilson KL** 2006 Barrier-to-autointegration factor-
765 like (BAF-L): a proposed regulator of BAF. *Experimental Cell Research* **312** 478–487.
- 766 **Tschiya Y, Hase A, Ogawa M, Yorifuji H & Arahata K** 1999 Distinct regions specify the

LEM-domain proteins during human spermiogenesis

12/06/2017

32

- 767 nuclear membrane targeting of emerin, the responsible protein for Emery-Dreifuss muscular
768 dystrophy. *European Journal of Biochemistry / FEBS* **259** 859–865.
- 769 **Ulbert S, Antonin W, Platani M & Mattaj IW** 2006 The inner nuclear membrane protein
770 Lem2 is critical for normal nuclear envelope morphology. *FEBS Letters* **580** 6435–6441.
- 771 **World Health Organisation** 2009 *WHO laboratory manual for the examination of human*
772 *semen and sperm-cervical mucus interaction*, Cambridge University Press, Cambridge.
- 773 **Worman HJ, Yuan J, Blobel G & Georgatos SD** 1988 A lamin B receptor in the nuclear
774 envelope. *Proceedings of the National Academy of Sciences of the United States of America*
775 **85** 8531–8534.
- 776 **Yassine S, Escoffier J, Abi Nahed R, Nahed RA, Pierre V, Karaouzene T, Ray PF &**
777 **Arnoult C** 2015 Dynamics of Sun5 localization during spermatogenesis in wild type and
778 Dpy19l2 knock-out mice indicates that Sun5 is not involved in acrosome attachment to the
779 nuclear envelope. *PloS One* **10** e0118698.
- 780 **Ye Q & Worman HJ** 1994 Primary structure analysis and lamin B and DNA binding of
781 human LBR, an integral protein of the nuclear envelope inner membrane. *The Journal of*
782 *Biological Chemistry* **269** 11306–11311.
- 783 **Ye Q, Callebaut I, Pezhman A, Courvalin JC & Worman HJ** 1997 Domain-specific
784 interactions of human HP1-type chromodomain proteins and inner nuclear membrane protein
785 LBR. *The Journal of Biological Chemistry* **272** 14983–14989.
- 786 **Yuki D, Lin Y-M, Fujii Y, Nakamura Y & Furukawa Y** 2004 Isolation of LEM domain-
787 containing 1, a novel testis-specific gene expressed in colorectal cancers. *Oncology Reports*
788 **12** 275–280.
- 789 **Zheng R, Ghirlando R, Lee MS, Mizuuchi K, Krause M & Craigie R** 2000 Barrier-to-
790 autointegration factor (BAF) bridges DNA in a discrete, higher-order nucleoprotein complex.
791 *Proceedings of the National Academy of Sciences of the United States of America* **97** 8997–

LEM-domain proteins during human spermiogenesis

12/06/2017

33

792 9002.

793 **Zhu F, Wang F, Yang X, Zhang J, Wu H, Zhang Z, Zhang Z, He X, Zhou P, Wei Z et al.**

794 2016 Biallelic SUN5 Mutations Cause Autosomal-Recessive Acephalic Spermatozoa

795 Syndrome. *American Journal of Human Genetics* **99** 942-949.796 **Zierhut C, Jenness C, Kimura H & Funabiki H** 2014 Nucleosomal regulation of chromatin797 composition and nuclear assembly revealed by histone depletion. *Nature Structural &*798 *Molecular Biology* **21** 617–625.

799

For Review Only

Figure and Table Legends

Figure 1. RT-PCR amplification of transcripts coding LEM-Domain proteins in human from total spermatozoa RNA, testis RNA and skeletal muscle RNA. RT-PCR analysis of the 5' and 3' ends of the coding region were performed separately for all tested transcripts, except for the short two exon coding regions of BAF and BAF-L which were tested with a single RT-PCR assay. RT-PCR products are shown migrated on a 3% agarose gel. Spermatozoa RNAs were extracted from samples from individuals 1-5 in Table 1. The protein encoded by the target transcript and the primer pairs used are indicated at the right of the gel. The known spermatid transcript for protamine 1 (PRM1) was amplified as a positive control. The expected size of each amplicon is shown at the left of the gel. The ladder is 1 kb Plus DNA Ladder (Life Technologies), and the 200 bp band is indicated with an (*).

Figure 2. RT-PCR analysis of mouse transcripts for LEMD1 and BANF2 on RNA extracted from staged mouse testis of different postnatal ages (*dpp*: days *post partum*). The expected germ cell content is indicated above the gel by the grey bars. Amplicons from LEMD1 or BAF-L transcripts were co-amplified with amplicons from the control HMBS transcript by RT-PCR, and show that LEMD1 and BANF2 transcripts predominate during mouse spermiogenesis. The proteins encoded by transcripts and the primers pair used are indicated at the right of the gel. The expected sizes of amplicons are shown at the left of the gel. The ladder is 1 kb Plus DNA Ladder (Life Technologies), and the 200 bp band is indicated with an (*).

Figure 3. An alternative ANKLE2 transcript encoding ANKLE2_Δ1 -64 is present in spermatids. (A) Schematic representation of full length ANKLE2 isoform described in databases, and a testis EST (HY008086) that includes an alternative first exon in intron 1. (B)

Specific RT-PCR analysis of the human transcripts encoding the two ANKLE2 isoforms from spermatozoa RNA (individuals 1-5 in Table 1), testis RNA and skeletal muscle RNA. (C) RT-PCR analysis of the novel alternative transcript ANKLE2_Δ1-64 in six tissues: brain, small intestine, skeletal muscle, prostate, thymus and testis. (B and C) PCR products were migrated on 3% agarose gel. The protein encoded by the target transcripts and the primer pairs used are indicated at to the right of the gel. The expected size of amplicon is shown at the left of the gel. The ladder is 1 kb plus (Life Technologies), and the 200 bp band is indicated with an (*).

Figure 4 . ANKLE2 full-length isoform, but not ANKLE2_Δ1-64, co-localises with the ER-marker GRP94 in HeLa cells and in spermatids. (A) Expression of ANKLE2-Flag and ANKLE2_Δ1-64-Flag (green) in HeLa cells, showing a granular aspect throughout the cytoplasm for ANKLE2 full length and GRP94 (red), with a strong overlap between ANKLE2 full length and GRP94 (yellow in MERGE photos). On the contrary, ANKLE2_Δ1-64 shows a more homogeneous cytoplasmic distribution and little overlap with the GRP94 signal. (B) Immunolocalisation of ANKLE2 on human spermatids, testicular spermatozoa and somatic cells. Spermatids and spermatozoa are identified by the labelling of acrosomes with an anti-SPACA1 antibody (violet). Extensive overlap of ANKLE2 (green) and GRP94 (red) signals is seen in round spermatids (yellow in MERGE), reduced overlap in elongated spermatids and no labelling in testicular spermatozoa. DNA is counterstained with DAPI (blue). Scale bar is 10 μm.

Figure 5. An alternative transcript for LEMD2 is present in spermatids. (A) Schematic representation of LEMD2 full length isoform with the position of primers used in RT-PCR analyses and the cryptic splice site that leads to the alternative transcript encoding

LEMD2_Δ115 -259. Primer o5055 is specific for the LEMD2_Δ115 -259 transcript. Primers o4711 and o4712 were used to amplify the full coding region from testis RNA and generated two bands (right panel) that were sequenced and the predicted proteins encoded by these transcripts are represented schematically with the different domains (TM: transmembrane) mapped to LEMD2 (Brachner *et al.*, 2005). **(B)** RT-PCR analysis of the alternative transcript encoding LEMD2_Δ115 -259 in human spermatozoa (individuals 1-5 in Table 1), and six tissues: brain, small intestine, skeletal muscle, prostate, thymus and testis. PCR products were migrated on 3% agarose gels. The ladder is 1 kb plus (Life technologies), and the 200 bp band is indicated with an (*). **(C)** Ectopic expression of fusion proteins LEMD2 and LEMD2_Δ115 -259 (green) with C-terminal Flag tag (red) in HeLa cells. Only LEMD2 transfected cells were labelled with anti-LEMD2 (Sigma HPA017340), indicating that this antibody is specific for the full-length isoform of LEMD2. Scale bar is 10 μm.

Figure 6. Immunolocalisation of LEM-domain proteins and BAF proteins (green) on human spermatids and testicular spermatozoa. Labelling is shown on successive steps of spermatid development: early, mid and late round, early elongating and testicular spermatozoa. The antibodies used are indicated in green. Spermatids are identified using lectin PNA (red) and DNA counterstained with DAPI (blue). Exposures have been normalised on Sertoli cell labelling. Scale bar is 10 μm.

Figure 7. Immunolocalisation of BAF and BAF-L on human ejaculated spermatozoa. **(A)** Composite montage of spermatozoa labelled with BAF and BAF-L (green). BAF and BAF-L were detected respectively in 30% and 36,9% of mature ejaculated spermatozoa, at the posterior pole of the nucleus (upper panels). No labelled spermatozoa were observed when each antibody was pre-absorbed with its immunogen peptide (lower panels). Acrosomes were

labelled using lectin PNA (red) and the nucleus is stained with DAPI (blue). Scale bar is 10 μm . **(B)** Protein expression of BAF and BAF-L by western blot analysis of human spermatozoa lysates. Results are shown for human testis (T011400051, T011500055, T011400062 and T011400071) (20 μg) and three spermatozoa samples (2×10^6 spermatozoa) corresponding to individuals 11-13 in Table 1. The anti- α tubulin antibody was used, on the same membranes without prior stripping, as a loading control. In order to reveal the faint signal of BAF-L in whole testis lysates, a long exposure of a segment of the BAF-L blot (between the grey bars) was compressed vertically and is shown below the α -tubulin result.

Table 1: Sperm parameters of patients whose spermatozoa were used for RT-PCR, western blot (WB), immunofluorescence analysis (IF) and selection procedures. ^F Fertile patients, ^{SI} Secondary infertility, *WHO criteria, **Normal forms (David criteria).

Table 2: The presence (+) or absence (-) of LEM-domain proteins, BAF proteins, LBR and lamins, and their respective transcripts in human spermatids and spermatozoa, as determined by us in this study or previously (Elkhatib *et al.* 2015). nd: not determined; +?: the absence of an antibody that discriminates between lamin B2 and lamin B3 prevents us from determining which is present.

Supplementary data Figure Legends

Figure S1: Phase contrast overlay on IF analysis of testicular cells and HeLa cells used for the localisation of ANKLE2.

Figure S2: Affinity tests of antibodies used in immunofluorescence analyses. LEM-domain proteins and BAF proteins (green) tagged with c-Myc or Flag (red) were ectopically expressed in HeLa cells. Tagged proteins were detected using antibodies against the target protein (green) and against the tag (red). The anti-LAP2 β antibody was tested on HeLa cells transfected with a construct expressing tagged versions of either LAP2 α (nucleoplasm) or LAP2 β (nuclear periphery), and its failure to label the nucleoplasm in LAP2 α transfected cells shows the antibody does not have high affinity for native LAP2 α . DNA is counterstained with DAPI (blue). Scale bar is 10 μ m.

Figure S3: Immunolocalisation of LEM-domain proteins on human spermatids, testicular spermatozoa and somatic cells showing the difference of localisation of different proteins (green) between germ cells and somatic cells. Spermatids are identified using lectin PNA (red) and counterstained with DAPI (blue). Exposures for the different antibodies were normalised on Sertoli cell labelling. Scale bar is 10 μ m.

Figure S4: Western blot analysis of protein lysates from human testis and purified spermatozoa with the anti-Emerin antibody Sigma AMAb90560. The predicted molecular weight of Emerin is 29 kDa.

Figure S5: Immunolocalisation of LEMD3, LBR, LEMD2 on cells from disaggregated human testis. Spermatids and testicular spermatozoa are not labelled, only somatic cells are labelled (green) with anti-LEMD3 (ab123973), anti-LBR (ab32535) and anti-LEMD2-mid antibody (Sigma HPA017340). The LEMD2-mid antibody is specific for the full LEMD2 isoform. Spermatids are identified using lectin PNA (red) and DNA is counterstained with

DAPI (blue). Exposures for the different antibodies were normalised on Sertoli cell labelling. Scale bar is 10 μ m.

Figure S6: Immunolocalization of Emerin on cells from disaggregated human testis and ejaculated spermatozoa. Spermatids and spermatozoa are not labelled, only somatic cells are labelled (green) with two different anti-Emerin antibodies (LEICA-NCL-EMERIN and Sigma AMAb90560 - green). Ejaculated spermatozoa are presented in a composite montage. Spermatids are identified using lectin PNA (red) and DNA is counterstained with DAPI (blue). Exposures for the two antibodies were normalised on Sertoli cell labelling. Scale bar is 10 μ m.

Figure S7: (A) Percentages of germ cells labelled with anti-BAF antibody (ab129184) (green) on post-meiotic germ cells of 4 patients (T011400051, T011400063, T011400071 and T011500055). (B) Three examples of the labelling round spermatids, elongating spermatids and testicular spermatozoa with the anti-BAF antibody (green). Nuclei are labelled with DAPI (blue) and acrosomes with lectin PNA (red). (C) Immunofluorescent labelling of BAF (green) on three spermatocytes. DNA is counterstained with DAPI (blue).

Table S1: Primer sequences used in RT-PCR, DNA constructs and sequencing. Adaptors used for constructs are underlined and the name of the restriction enzyme site in the adaptor is preceded by a + after the target gene name. Target gene prefix: h=human; m=mouse.

Table S2: Antibodies used in immunofluorescence and western blot analyses. For primary antibodies, IF and Western tests refer to affinity tests by transfection into tissue culture cells

(Figure S1). For secondary antibodies, this refers to the absence of IF signal when antibody is used without a primary antibody.

For Review Only

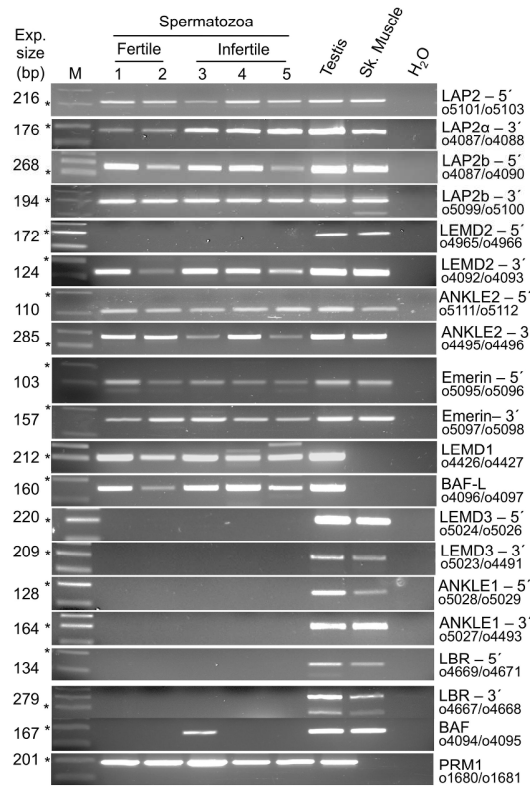


Figure 1. RT-PCR amplification of transcripts coding LEM-Domain proteins in human from total spermatozoa RNA, testis RNA and skeletal muscle RNA. RT-PCR analysis of the 5' and 3' ends of the coding region were performed separately for all tested transcripts, except for the short two exon coding regions of BAF and BAF-L which were tested with a single RT-PCR assay. RT-PCR products are shown migrated on a 3% agarose gel. Spermatozoa RNAs were extracted from samples from individuals 1-5 in Table 1. The protein encoded by the target transcript and the primer pairs used are indicated at the right of the gel. The known spermatid transcript for protamine 1 (PRM1) was amplified as a positive control. The expected size of each amplicon is shown at the left of the gel. The ladder is 1 kb Plus DNA Ladder (Life Technologies), and the 200 bp band is indicated with an (*).

Figure 1. RT-PCR amplification of transcripts coding LEM-Domain proteins in human from total spermatozoa RNA, testis RNA and skeletal muscle RNA. RT-PCR analysis of the 5' and 3' ends of the coding region were performed separately for all tested transcripts, except for the short two exon coding regions of BAF and BAF-L which were tested with a single RT-PCR assay. RT-PCR products are shown migrated on a 3% agarose gel. Spermatozoa RNAs were extracted from samples from individuals 1-5 in Table 1. The protein encoded by the target transcript and the primer pairs used are indicated at the right of the gel. The known spermatid transcript for protamine 1 (PRM1) was amplified as a positive control. The expected size of each amplicon is shown at the left of the gel. The ladder is 1 kb Plus DNA Ladder (Life Technologies), and the 200 bp band is indicated with an (*).

228x302mm (300 x 300 DPI)

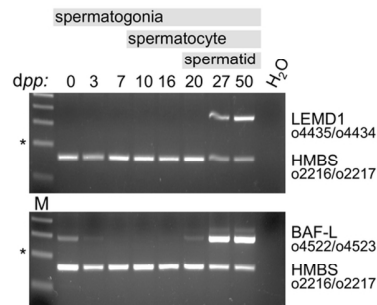


Figure 2. RT-PCR analysis of mouse transcripts for LEMD1 and BANF2 on RNA extracted from staged mouse testis of different postnatal ages (*dpp*: days post partum). The expected germ cell content is indicated above the gel by the grey bars. Amplicons from LEMD1 or BAF-L transcripts were co-amplified with amplicons from the control HMBS transcript by RT-PCR, and show that LEMD1 and BANF2 transcripts predominate during mouse spermiogenesis. The proteins encoded by transcripts and the primers pair used are indicated at the right of the gel. The expected sizes of amplicons are shown at the left of the gel. The ladder is 1 kb Plus DNA Ladder (Life Technologies), and the 200 bp band is indicated with an (*).

Figure 2. RT-PCR analysis of mouse transcripts for LEMD1 and BANF2 on RNA extracted from staged mouse testis of different postnatal ages (*dpp*: days post partum). The expected germ cell content is indicated above the gel by the grey bars. Amplicons from LEMD1 or BAF-L transcripts were co-amplified with amplicons from the control HMBS transcript by RT-PCR, and show that LEMD1 and BANF2 transcripts predominate during mouse spermiogenesis. The proteins encoded by transcripts and the primers pair used are indicated at the right of the gel. The expected sizes of amplicons are shown at the left of the gel. The ladder is 1 kb Plus DNA Ladder (Life Technologies), and the 200 bp band is indicated with an (*).

109x68mm (300 x 300 DPI)

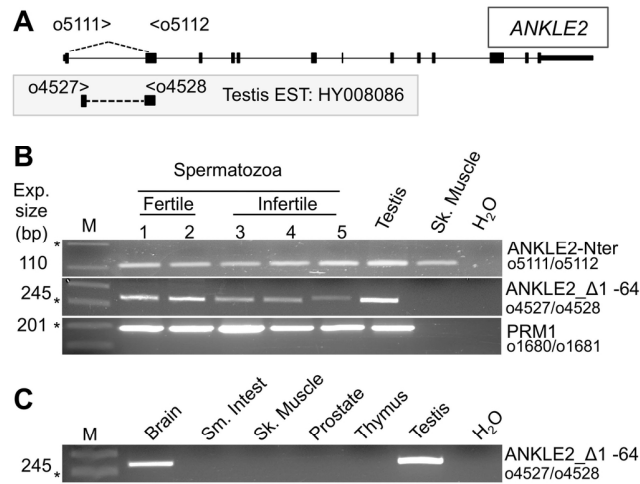


Figure 3. An alternative ANKLE2 transcript encoding ANKLE2_Δ1 -64 is present in spermatids. **(A)** Schematic representation of full length ANKLE2 isoform described in databases, and a testis EST (HY008086) that includes an alternative first exon in intron 1. **(B)** Specific RT-PCR analysis of the human transcripts encoding the two ANKLE2 isoforms from spermatozoa RNA (individuals 1-5 in Table 1), testis RNA and skeletal muscle RNA. **(C)** RT-PCR analysis of the novel alternative transcript ANKLE2_Δ1 -64 in six tissues: brain, small intestine, skeletal muscle, prostate, thymus and testis. **(B and C)** PCR products were migrated on 3% agarose gel. The protein encoded by the target transcripts and the primer pairs used are indicated at to the right of the gel. The expected size of amplicon is shown at the left of the gel. The ladder is 1 kb plus (Life Technologies), and the 200 bp band is indicated with an (*).

Figure 3. An alternative ANKLE2 transcript encoding ANKLE2_Δ1 -64 is present in spermatids. (A) Schematic representation of full length ANKLE2 isoform described in databases, and a testis EST (HY008086) that includes an alternative first exon in intron 1. (B) Specific RT-PCR analysis of the human transcripts encoding the two ANKLE2 isoforms from spermatozoa RNA (individuals 1-5 in Table 1), testis RNA and skeletal muscle RNA. (C) RT-PCR analysis of the novel alternative transcript ANKLE2_Δ1 -64 in six tissues: brain, small intestine, skeletal muscle, prostate, thymus and testis. (B and C) PCR products were migrated on 3% agarose gel. The protein encoded by the target transcripts and the primer pairs used are indicated at to the right of the gel. The expected size of amplicon is shown at the left of the gel. The ladder is 1 kb plus (Life Technologies), and the 200 bp band is indicated with an (*).

166x163mm (300 x 300 DPI)

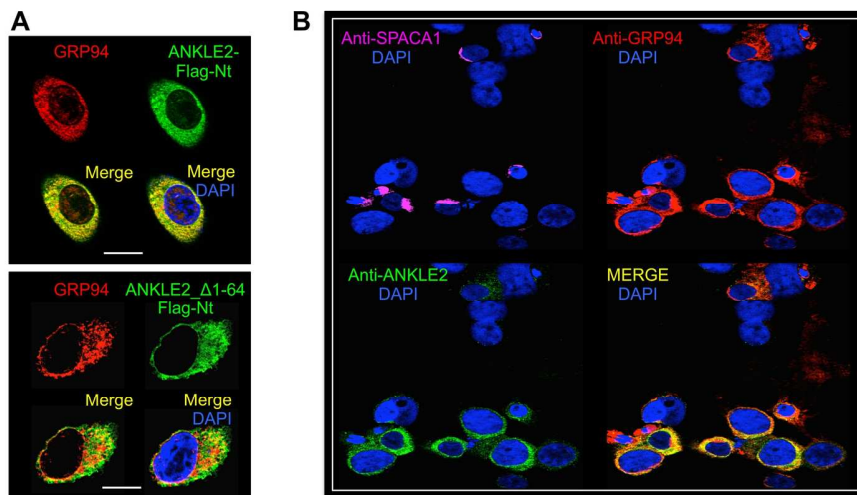


Figure 4 . ANKLE2 full-length isoform, but not ANKLE2_Δ1-64, co-localises with the ER-marker GRP94 in HeLa cells and in spermatids. (A) Expression of ANKLE2-Flag and ANKLE2_Δ1-64-Flag (green) in HeLa cells, showing a granular aspect throughout the cytoplasm for ANKLE2 full length and GRP94 (red), with a strong overlap between ANKLE2 full length and GRP94 (yellow in MERGE photos). On the contrary, ANKLE2_Δ1-64 shows a more homogeneous cytoplasmic distribution and little overlap with the GRP94 signal. (B) Immunolocalisation of ANKLE2 on human spermatids, testicular spermatozoa and somatic cells. Spermatids and spermatozoa are identified by the labelling of acrosomes with an anti-SPACA1 antibody (violet). Extensive overlap of ANKLE2 (green) and GRP94 (red) signals is seen in round spermatids (yellow in MERGE), reduced overlap in elongated spermatids and no labelling in testicular spermatozoa. DNA is counterstained with DAPI (blue). Scale bar is 10 microns.

Figure 4 . ANKLE2 full-length isoform, but not ANKLE2_Δ1-64, co-localises with the ER-marker GRP94 in HeLa cells and in spermatids. (A) Expression of ANKLE2-Flag and ANKLE2_Δ1-64-Flag (green) in HeLa cells, showing a granular aspect throughout the cytoplasm for ANKLE2 full length and GRP94 (red), with a strong overlap between ANKLE2 full length and GRP94 (yellow in MERGE photos). On the contrary, ANKLE2_Δ1-64 shows a more homogeneous cytoplasmic distribution and little overlap with the GRP94 signal. (B) Immunolocalisation of ANKLE2 on human spermatids, testicular spermatozoa and somatic cells. Spermatids and spermatozoa are identified by the labelling of acrosomes with an anti-SPACA1 antibody (violet). Extensive overlap of ANKLE2 (green) and GRP94 (red) signals is seen in round spermatids (yellow in MERGE), reduced overlap in elongated spermatids and no labelling in testicular spermatozoa. DNA is counterstained with DAPI (blue). Scale bar is 10 microns.

171x170mm (300 x 300 DPI)

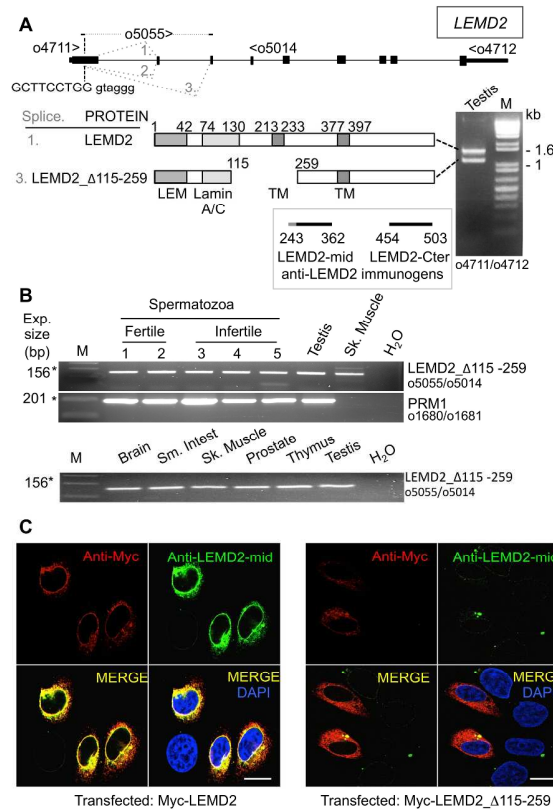


Figure 5. An alternative transcript for LEMD2 is present in spermatids. **(A)** Schematic representation of LEMD2 full length isoform with the position of primers used in RT-PCR analyses and the cryptic splice site that leads to the alternative transcript encoding LEMD2_Δ115-259. Primer o5055 is specific for the LEMD2_Δ115-259 transcript. Primers o4711 and o4712 were used to amplify the full coding region from testis RNA and generated two bands (right panel) that were sequenced and the predicted proteins encoded by these transcripts are represented schematically with the different domains (TM: transmembrane) mapped to LEMD2 (Brachner *et al.*, 2005). **(B)** RT-PCR analysis of the alternative transcript encoding LEMD2_Δ115-259 in human spermatozoa (individuals 1-5 in Table 1), and six tissues: brain, small intestine, skeletal muscle, prostate, thymus and testis. PCR products were migrated on 3% agarose gels. The ladder is 1 kb plus (Life technologies), and the 200 bp band is indicated with an (*). **(C)** Ectopic expression of fusion proteins LEMD2 and LEMD2_Δ115-259 (green) with C-terminal Flag tag (red) in HeLa cells. Only LEMD2 transfected cells were labelled with anti-LEM2 (Sigma HPA017340), indicating that this antibody is specific for the full-length isoform of LEMD2. Scale bar is 10 microns.

Figure 5. An alternative transcript for LEMD2 is present in spermatids. **(A)** Schematic representation of LEMD2 full length isoform with the position of primers used in RT-PCR analyses and the cryptic splice site that leads to the alternative transcript encoding LEMD2_Δ115-259. Primer o5055 is specific for the LEMD2_Δ115-259 transcript. Primers o4711 and o4712 were used to amplify the full coding region from testis RNA and generated two bands (right panel) that were sequenced and the predicted proteins encoded by these transcripts are represented schematically with the different domains (TM: transmembrane) mapped to LEMD2 (Brachner *et al.*, 2005). **(B)** RT-PCR analysis of the alternative transcript encoding LEMD2_Δ115-259 in human spermatozoa (individuals 1-5 in Table 1), and six tissues: brain, small intestine, skeletal muscle, prostate, thymus and testis. PCR products were migrated on 3% agarose gels. The ladder is 1 kb plus (Life technologies), and the 200 bp band is indicated with an (*). **(C)** Ectopic expression of fusion proteins LEMD2 and LEMD2_Δ115-259 (green) with C-terminal Flag tag (red) in HeLa cells. Only LEMD2 transfected cells were labelled with anti-LEM2 (Sigma HPA017340), indicating that this antibody is specific for the full-length isoform of LEMD2. Scale bar is 10 microns.

256x378mm (300 x 300 DPI)

For Review Only

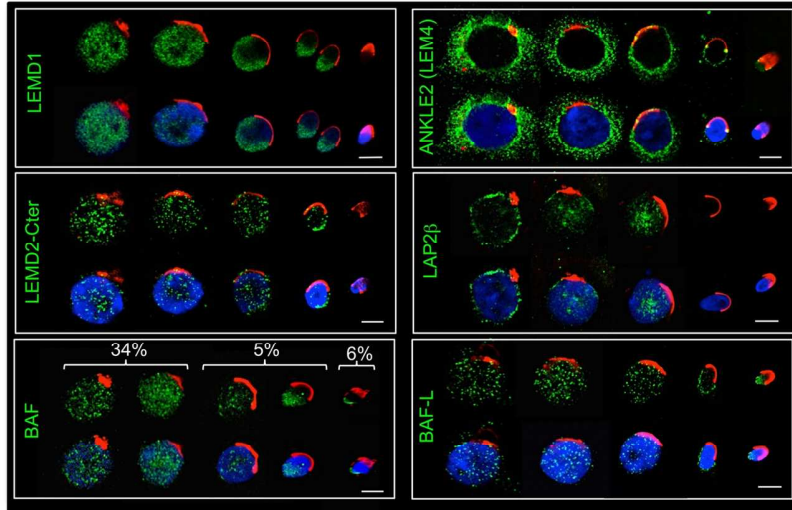


Figure 6. Immunolocalisation of LEM-domain proteins and BAF proteins (green) on human spermatids and testicular spermatozoa. Labelling is shown on successive steps of spermatid development: early, mid and late round, early elongating and testicular spermatozoa. The antibodies used are indicated in green. Spermatids are identified using lectin PNA (red) and DNA counterstained with DAPI (blue). Exposures have been normalised on Sertoli cell labelling. Scale bar is 10 μ m.

Figure 6. Immunolocalisation of LEM-domain proteins and BAF proteins (green) on human spermatids and testicular spermatozoa. Labelling is shown on successive steps of spermatid development: early, mid and late round, early elongating and testicular spermatozoa. The antibodies used are indicated in green. Spermatids are identified using lectin PNA (red) and DNA counterstained with DAPI (blue). Exposures have been normalised on Sertoli cell labelling. Scale bar is 10 μ m.

137x114mm (300 x 300 DPI)

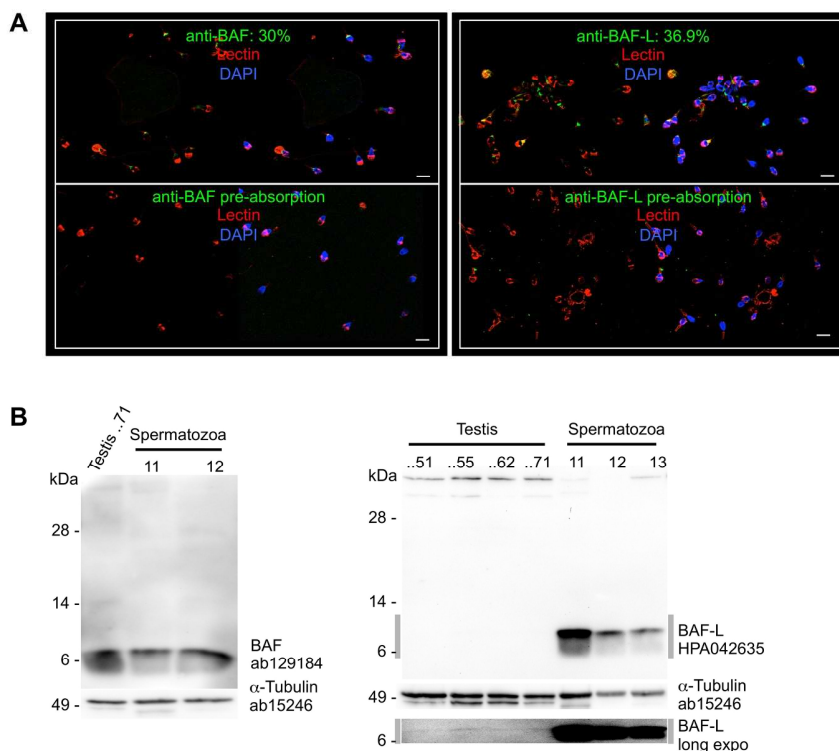


Figure 7. Immunolocalisation of BAF and BAF-L on human ejaculated spermatozoa. **(A)** Composite montage of spermatozoa labelled with BAF and BAF-L (green). BAF and BAF-L were detected respectively in 30% and 36.9% of mature ejaculated spermatozoa, at the posterior pole of the nucleus (upper panels). No labelled spermatozoa were observed when each antibody was pre-absorbed with its immunogen peptide (lower panels). Acrosomes were labelled using lectin PNA (red) and the nucleus is stained with DAPI (blue). Scale bar is 10 μ m. **(B)** Protein expression of BAF and BAF-L by western blot analysis of human spermatozoa lysates. Results are shown for human testis (T011400051, T011500055, T011400062 and T011400071) (20 μ g) and three spermatozoa samples (2×10^6 spermatozoa) corresponding to individuals 11-13 in Table 1. The anti- α tubulin antibody was used, on the same membranes without prior stripping, as a loading control. In order to reveal the faint signal of BAF-L in whole testis lysates, a long exposure of a segment of the BAF-L blot (between the grey bars) was compressed vertically and is shown below the α -tubulin result.

Figure 7. Immunolocalisation of BAF and BAF-L on human ejaculated spermatozoa. **(A)** Composite montage of spermatozoa labelled with BAF and BAF-L (green). BAF and BAF-L were detected respectively in 30% and 36.9% of mature ejaculated spermatozoa, at the posterior pole of the nucleus (upper panels). No labelled spermatozoa were observed when each antibody was pre-absorbed with its immunogen peptide (lower panels). Acrosomes were labelled using lectin PNA (red) and the nucleus is stained with DAPI (blue). Scale bar is 10 μ m. **(B)** Protein expression of BAF and BAF-L by western blot analysis of human spermatozoa lysates. Results are shown for human testis (T011400051, T011500055, T011400062 and T011400071) (20 μ g) and three spermatozoa samples (2×10^6 spermatozoa) corresponding to individuals 11-13 in Table 1. The anti- α -tubulin antibody was used, on the same membranes without prior stripping, as a loading control. In order to reveal the faint signal of BAF-L in whole testis lysates, a long exposure of a segment of the BAF-L blot (between the grey bars) was compressed vertically and is shown below the α -tubulin result.

206x245mm (300 x 300 DPI)

For Review Only

Patients	GT number	Spz (M/ml)	Motility (a+b/c/d)*	Vitality (%)	Normal forms ** (%)	Technics performed on spermatozoa
1 ^F	R 011300032	84	35/20/45	78	39	RT-PCR
2 ^F	R 011300029	160	50/10/40	70	37	RT-PCR, IF
3	R 010900491	102	45/20/35	85	45	RT-PCR, IF, WB
4 ^{SI}	R 010900544	150	50/20/30	80	41	RT-PCR
5	R 010900563	109.6	60/10/30	80	39	RT-PCR
6	R 01090026	44	60/20/20	64	20	RT-PCR
7	R 01090040	33,6	40/10/50	60	22	RT-PCR
8	R 010900236	63,4	30/25/40	81	20	RT-PCR
9	R 010900505	92	25/45/30	82	54	IF
10 ^F	R 011500066	135	30/10/60	65	22	WB
11 ^F	R 011500071	130	30/10/60	59	32	WB
12	R 010900549	195	60/10/30	85	53	WB
13	R 010900409	259,8	30/10/60	82	53	WB
14	R 010900214	159	35/10/55	70	34	WB

^F Fertile patients. ^{SI} Secondary infertility
 *WHO criteria, **Normal forms (David criteria)

	Transcript (RT-PCR)	Protein (IF)	
	Ejac. sperm.	Spermatid	Ejac. Sperm.
LEMD1	+	+	-
LEMD2-full	-	-	-
LEMD2- Δ 115-259	+	+	-
LEMD3	-	-	-
ANKLE2	+	+	-
ANKLE2_ Δ 1-64	+	nd	-
ANKLE1	-	nd	nd
LAP2 α	+	nd	nd
LAP2 β	+	+	-
Emerin	+	-	-
LBR	-	-	-
BAF	-	+	+ (30%)
BAF-L	+	+	+ (37%)
Lamin A	-	-	-
Lamin C	-	-	-
Lamin B1	+	+	+ (30-60%)
Lamin B2	-	+?	-
Lamin B3	+	+?	nd

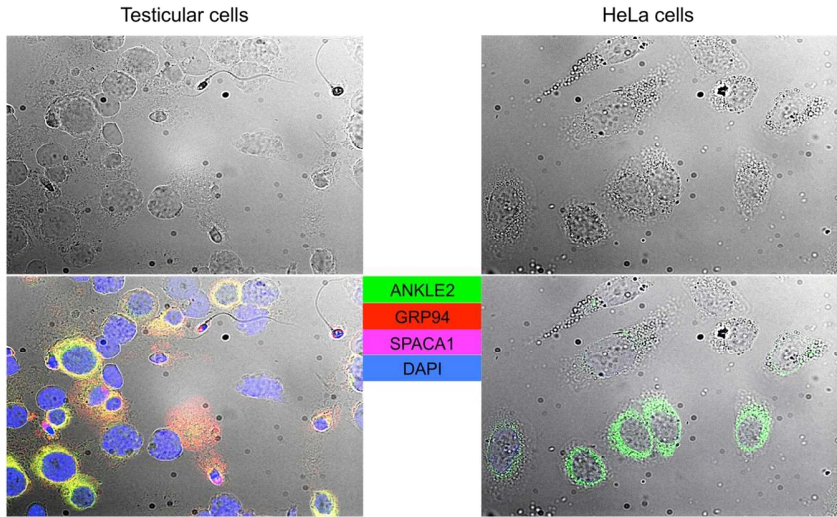


Figure S1. Phase contrast overlay on IF analysis of testicular cells and HeLa cells used for the localisation of ANKLE2.

129x97mm (300 x 300 DPI)

Only

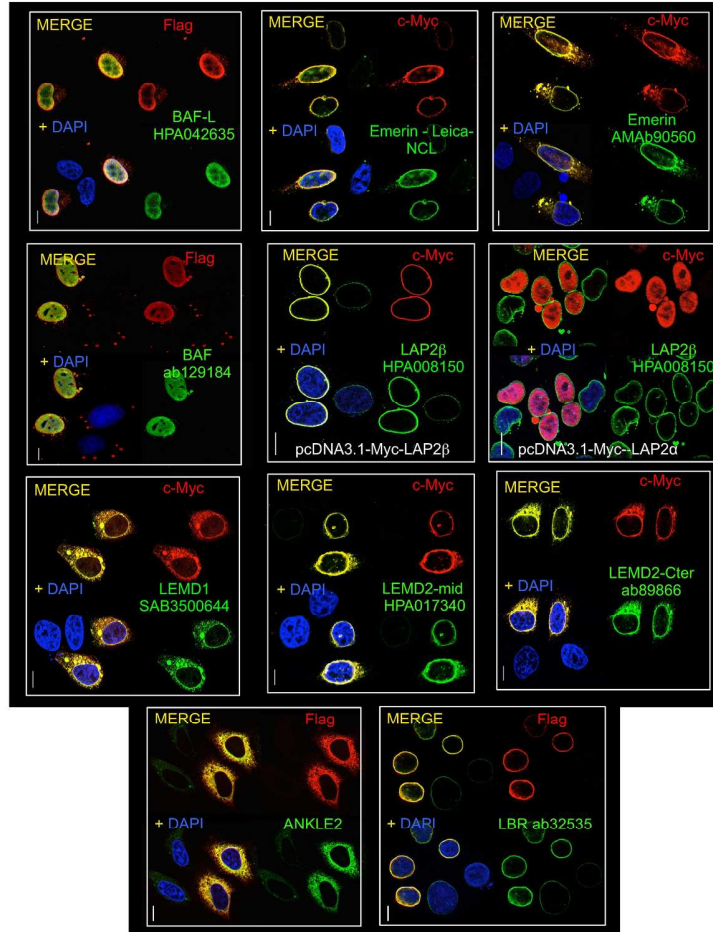


Figure S2. Affinity tests of antibodies used in immunofluorescence analyses. LEM-domain proteins and BAF proteins (green) tagged with c-Myc or Flag (red) were ectopically expressed in HeLa cells. Tagged proteins were detected using antibodies against the target protein (green) and against the tag (red). The anti-LAP2b antibody was tested on HeLa cells transfected with a construct expressing tagged versions of either LAP2a (nucleoplasm) or LAP2b (nuclear periphery), and its failure to label the nucleoplasm in LAP2a transfected cells shows the antibody does not have high affinity for native LAP2a. DNA is counterstained with DAPI (blue). Scale bar is 10 μ m.

215x268mm (300 x 300 DPI)

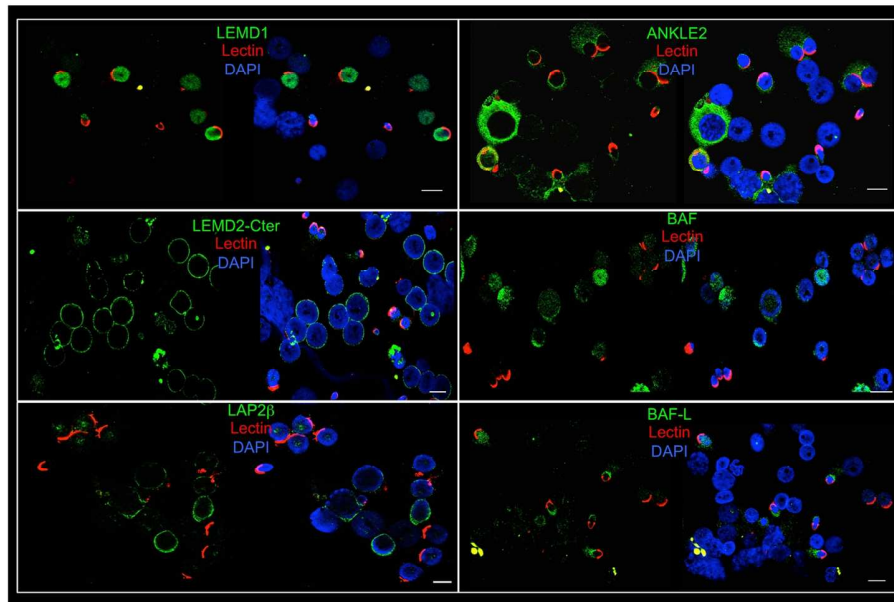


Figure S3: Immunolocalisation of LEM-domain proteins on human spermatids, testicular spermatozoa and somatic cells showing the difference of localisation of different proteins (green) between germ cells and somatic cells. Spermatids are identified using lectin PNA (red) and counterstained with DAPI (blue). Exposures for the different antibodies were normalised on Sertoli cell labelling. Scale bar is 10 μ m.

140x114mm (300 x 300 DPI)

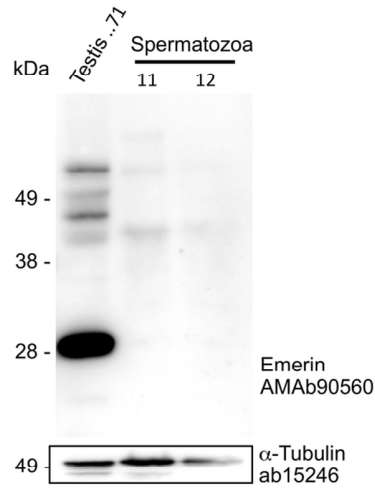


Figure S4. Western blot analysis of protein lysates from human testis and purified spermatozoa with the anti-Emerin antibody Sigma AMAb90560. The predicted molecular weight of Emerin is 29 kDa.

105x74mm (300 x 300 DPI)

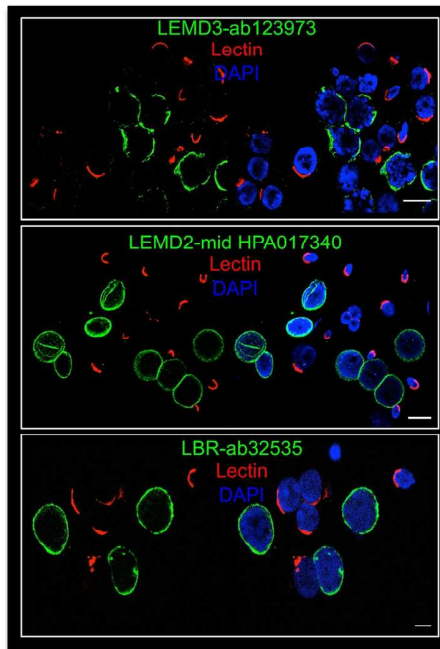


Figure S5. Immunolocalisation of LEMD3, LBR, LEMD2 on cells from disaggregated human testis. Spermatids and testicular spermatozoa are not labelled, only somatic cells are labelled (green) with anti-LEMD3 (ab123973), anti-LBR (ab32535) and anti-LEMD2-mid antibody (Sigma HPA017340). The LEMD2-mid antibody is specific for the full LEMD2 isoform. Spermatids are identified using lectin PNA (red) and DNA is counterstained with DAPI (blue). Exposures for the different antibodies were normalised on Sertoli cell labelling. Scale bar is 10 μm .

154x150mm (300 x 300 DPI)

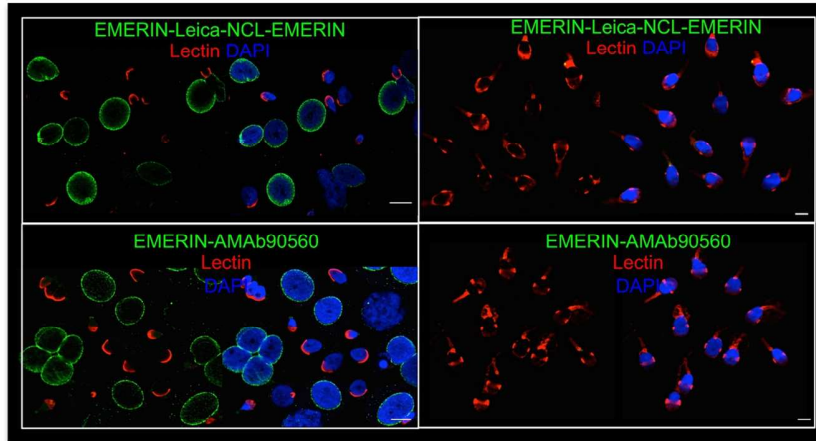
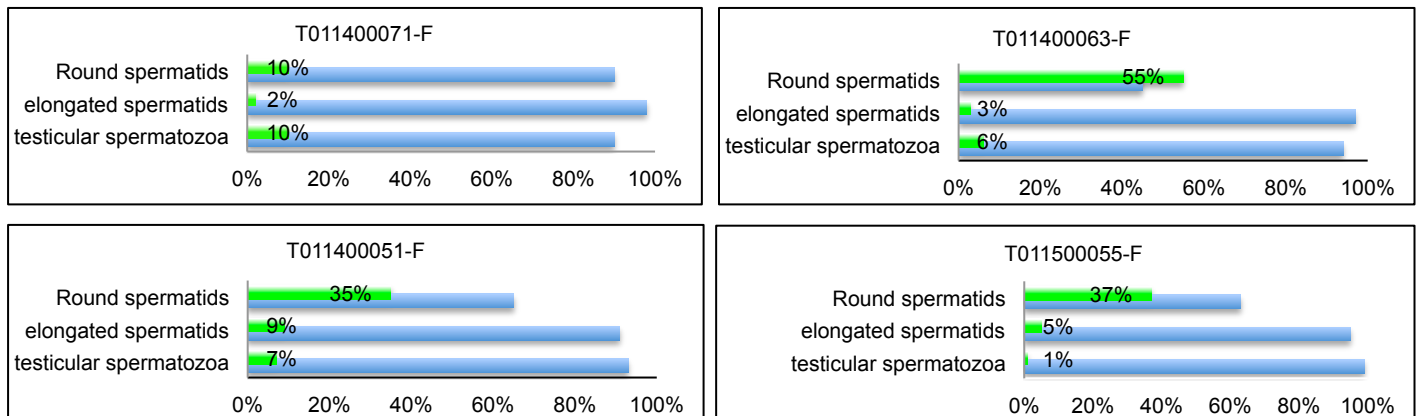


Figure S6. Immunolocalization of Emerin on cells from disaggregated human testis and ejaculated spermatozoa. Spermatids and spermatozoa are not labelled, only somatic cells are labelled (green) with two different anti-Emerin antibodies (LEICA-NCL-EMERIN and Sigma AMAb90560 - green). Ejaculated spermatozoa are presented in a composite montage. Spermatids are identified using lectin PNA (red) and DNA is counterstained with DAPI (blue). Exposures for the two antibodies were normalised on Sertoli cell labelling. Scale bar is 10 μ m.

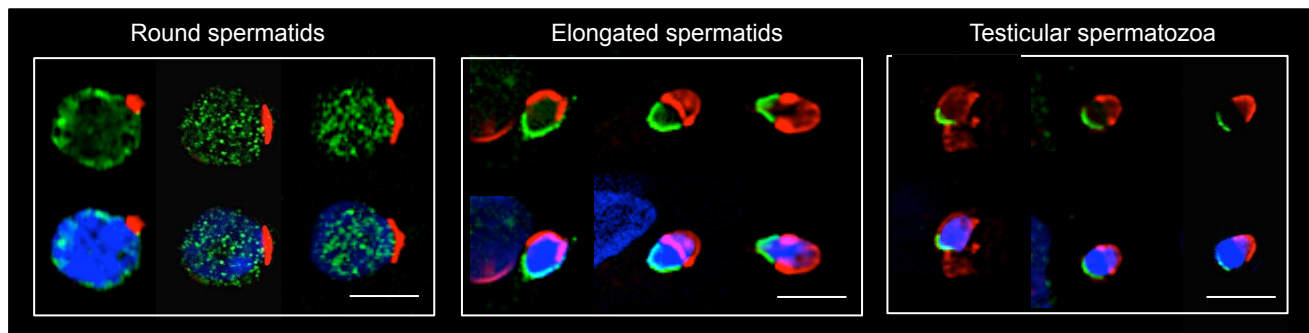
122x92mm (300 x 300 DPI)

Only

A



B



C

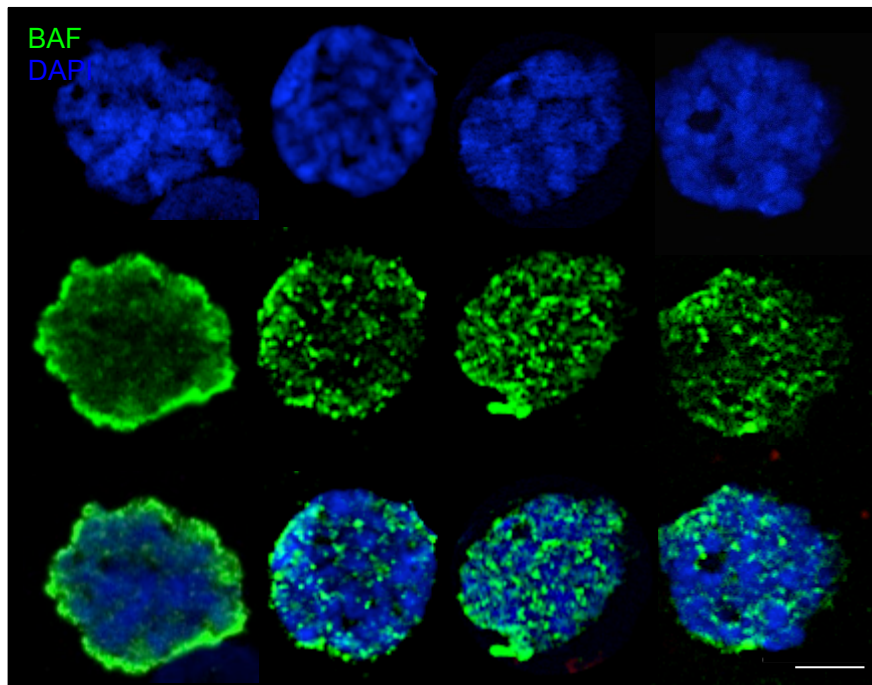


Figure S7. (A) Percentages of germ cells labelled with anti-BAF antibody (ab129184) (red) on post-meiotic germ cells of 4 patients (T011400051, T011400063, T011400071 and T011500055). **(B)** Three examples of the labelling on round spermatids, elongating spermatids and testicular spermatozoa with the anti-BAF antibody (green). Nuclei are labelled with DAPI (blue) and acrosomes with lectin (red). **(C)** Immunofluorescent labelling of BAF (green) on a spermatocyte. DNA is counterstained with DAPI (blue). Scale bar is 10 μ m.

Primer number	Primer sequence	Target Gene	Annealing temperature
o1680	AGGTACAGATGCTGTCGCAG	h_PRM1	65°C
o1681	AGTCTGGTAACATTCTCAGGC	h_PRM1	62°C
o2216	TGAAAGCCTTGTACCCTGGC	m_Hmbs	66°C
o2217	GAGTGAACGACCAGGTCCAC	m_Hmbs	66°C
o4087	TCTTCTACTCCTCTGCCAAC	h_TMPO (LAP2)	61°C
o4088	CCACCAGAGGGAGTAGTTCC	h_TMPO (LAP2 α)	65°C
o4090	GTTAATGCCTGCAGAGGTCC	h_TMPO (LAP2 β)	64°C
o4092	TCCAGGACCATTACGTGGAC	h_LEMD2	65°C
o4093	CTCGGTCCCAGACACGCTTC	h_LEMD2	69°C
o4094	TTGGTGAAGTCTGGGCAAG	h_BANF1	66°C
o4095	GAAGGCATCCGAAGCAGTCC	h_BANF1	67°C
o4096	TGGGTGGATGGCATCAGCC	h_BANF2	69°C
o4097	CCTCACACTCAGTGGCACC	h_BANF2	66°C
o4367	<u>AGGTTCGAATTCGCTAGCGAGATGGACGACATGTCTCC</u>	h_BANF2 +NheI	63°C
o4368	<u>ATTTGACGGATCCAGGAAGCAGGCACACCAC</u>	h_BANF2 +BamHI	67°C
o4388	<u>AGGTTCGAATTCGCTAGCGATCAAGATGACAACCTCCC</u>	h_BANF1 +EcoRI-NheI	62°C
o4389	<u>ATTTGACGGATCCTCACAAGAAGGCGTCGCACC</u>	h_BANF1 +BamHI	69°C
o4399	<u>ATTTGACGGATCCCAAGAAGGCGTCGCACCAC</u>	h_BANF1 +BamHI	70°C
o4426	GCCCAATACTACCTTCCACC	h_LEMD1	63°C
o4427	AAGCCTCAGGCCATTTTTGAG	h_LEMD1	64°C
o4434	GCCTCAAGTCTCTTCTTGCC	m_Lemd1	64°C
o4435	GATTGCATAGACTTCAGACAACC	m_Lemd1	61°C
o4491	GGCTTCAATGGAGTGTGGGA	h_LEMD3	63°C
o4493	CATAGCAGTGCCTTGCTTC	h_ANKLE1	64°C
o4495	ATGTCCTTGAGTCCCAGCAG	h_ANKLE2	65°C
o4496	ACTGAGATCTGGCAGCTGAG	h_ANKLE2	65°C
o4500	AACCATGATTGCAGACATTG	h_ANKLE2	59°C
o4501	CCCTCACGGAAATGGAATTG	h_ANKLE2	62°C
o4502	CATGAGCTGGGGTATCCCTG	h_ANKLE2	66°C
o4503	AGTTCGAGACCAGCCTGGTC	h_ANKLE2	67°C
o4504	GGAAAACCTCACCTCGAGAG	h_ANKLE2	63°C
o4522	<u>AGGTCTCATATGAAGATGGACGACATGTCGCC</u>	m_Banf2	66°C
o4523	<u>TTTGACGAATTCTTAGGAAACAGGAGCACCCT</u>	m_Banf2	64°C
o4527	CGGTAGACTGTCGGGTCTGG	h_ANKLE2	68°C
o4528	AGAGCTGTGACACCTGCCTC	h_ANKLE2	68°C
o4542	<u>TTGGCAGGTACCGAAATGACAATGGATGCTCTGTTGG</u>	h_ANKLE2_Δ1-64 +KpnI	65°C
o4573	<u>TTGGCAGGTACCATGCTGTGGCCGCGGCTGG</u>	h_ANKLE2 +KpnI	65°C
o4579	<u>ATTGCAGGATCCGACAACCTACGCAGATCTTTCGG</u>	h_EMD +BamHI	67°C

o4580	<u>ATTGAACTCGAGT</u> CATGGCTCCCTCTAGAAGG	h_EMD +XhoI	64°C
o4609	AAAGTGCTCCTCCAAGCCAG	h_PTPRC	59°C
o4610	GCCAGAAATGCTATCAGTGCCTTAG	h_PTPRC	60°C
o4611	GCTTCGCGTCCAGACAGG	h_KIT	61°C
o4612	CGTGTATTTGCCGGTGTGG	h_KIT	59°C
o4613	CTTTGACGCCGAGAGCTACA	h_CDH1	59°C
o4614	TTTGAATCGGGTGTGAGGG	h_CDH1	59°C
o4615	<u>ATGCTCCTCGAGC</u> CAATTCAGTTGGATTTCTAGGGTCAAC	h_TMPO (LAP2 β) +XhoI	66°C
o4659	<u>ATGGTCCTCGAGT</u> TAACCAAACAGCGACTTATTTTC	h_LEMD1 +XhoI	59°C
o4661	<u>AGGTCTGGTACC</u> ATGGTGGATGTGAAGTGTCTG	h_LEMD1 +KpnI	63°C
o4663	<u>CCTAGACTCGAGC</u> TACAGGAAGCAGGCACACCAC	h_BANF2 +XhoI	71°C
o4667	CTGTCGCTGCCAGCTCTG	h_LBR	70°C
o4668	GGATGATGTCCATGGTCGTC	h_LBR	63°C
o4669	ACCGAGCCCTCCTCGCAG	h_LBR	72°C
o4671	GGGAGGTGCTGTCGTGGCTC	h_LBR	72°C
o4702	<u>GGTTATAAGCTT</u> AACAACCTCCAAAAGCACC	h_BANF1 +HindIII	64°C
o4710	<u>AGGTCAGGATCC</u> CTACAGGGCGGCAAGCTCA	h_ANKLE2 +BamHI	68°C
o4711	<u>ATGGCTAAGCTT</u> GCCGGCCTGTCGGACCT	h_LEMD2 +HindIII	72°C
o4712	<u>TTGGCAGGTACC</u> GGGGCTTATCGCTCTGAGTC	h_LEMD2 +KpnI	70°C
o4965	GCTACTGCTCGTCTTCCTGG	h_LEMD2	66°C
o4966	GTAGAGTTCATGCAGCAGCTC	h_LEMD2	64°C
o5022	<u>ATCCGGGATCC</u> CGGAGTTCCTGGAAGACC	h_TMPO (LAP2 β) +BamHI	66°C
o5023	GACACCGTGTCTAAAGATTCGG	h_LEMD3	63°C
o5024	GTGCCCACTACTGTGCATG	h_LEMD3	64°C
o5026	GCAAGCTGTGCCAATCGATCA	h_LEMD3	67°C
o5027	CAAGGTGCGTCAGATCTTGG	h_ANKLE1	64°C
o5028	AATCGACCGACCAGGCGGTG	h_ANKLE1	71°C
o5029	AGCGCAGCAGCTCCTCTACT	h_ANKLE1	69°C
o5095	CCGAGCTGACCACCTTGCTG	h_EMD	69°C
o5096	CTGGGTCTCGTACTCGAAGAT	h_EMD	64°C
o5097	GCTGTCCGCCAGTCAGTGAC	h_EMD	69°C
o5098	GGTAGTGCCTGATGCTCTGG	h_EMD	66°C
o5099	AGCATGCATCTCCTATTCTGCC	h_TMPO (LAP2 β)	65°C
o5100	GATTGGTCTGCGGCAACTAGCA	h_TMPO (LAP2 β)	67°C
o5101	CGGACTTCTCCAGTGACGAAGAG	h_TMPO (LAP2)	67°C
o5103	CCACAATAGGACCAGGATCACTCC	h_TMPO (LAP2)	67°C
o5111	CCCCGCCTCAGGTGAAATG	h_ANKLE2	69°C
o5112	GGGTCCACATTTCAATCCGGCTTTG	h_ANKLE2	69°C
o5186	<u>GGTTATAAGCTT</u> GACGACATGTCTCCAGGCTG	h_BANF2 +HindIII	70°C

o5322	<u>ATGGCTAAGCTT</u> ATGGCCGGCCTGTCGGACCT	h_LEMD2 +HindIII	78°C
o5323	<u>TTGGCAGGTACCT</u> CGCTCTGAGTCAGAGAAGG	h_LEMD2 +KpnI	66°C
o5350	<u>ATTTGACCATATG</u> TTCTCTCCGAACCCATTGGAG	h_BANF2 +NdeI	69°C
o5351	<u>ATTTGACCTCGAG</u> CAGGAAGCAGGCACACCAC	h_BANF2 +XhoI	69°C
o5352	<u>GTTCCAGGTACCA</u> TGCCAAGTAGGAAATTTGCCGATG	h_LBR +KpnI	68°C
o5353	<u>AAGTCCGGATCCG</u> TAGATGTATGGAAATATACGGTAGGGCAC	h_LBR +BamHI	68°C
o5354	<u>GTTCCAGGTACCC</u> CAAGTAGGAAATTTGCCGATGGTG	h_LBR +KpnI	68°C
o5355	<u>AAGTCCGGATCC</u> TTAGTAGATGTATGGAAATATACGGTAGGGCAC	h_LBR +BamHI	68°C

Table S1. Primer sequences used in RT-PCR, DNA constructs and sequencing. Adaptors used for constructs are underlined and the name of the restriction enzyme site in the adaptor is preceded by a + after the target gene name. Target gene prefix: h=human; m=mouse.

Antibodies	References	Epitope or immunogen position	IF tests	WB tests
LEMD1	Sigma SAB3500644	aa 80-130 in isoform 1 (181 aa)	YES	YES
LEMD2_mid	Sigma HPA017340	aa 243-359 (this study)	YES	NO
LEMD2-C-ter	ab89866	aa 454-503	YES	YES (by abcam)
LEMD3	ab123973	Within human LEMD3	YES (by abcam)	YES (by abcam)
ANKLE2	Asencio et al., 2012	aa 59-938	YES	YES
Emerin	Leica-NCL-EMERIN	222 amino acid region near N-terminus	YES	Not recommended
Emerin	Sigma AMAb90560	63-DALLYQSKGYNDYY-77	YES	NO
LAP2 \square	sigma HPA008150	aa 129-187 (this study)	YES	YES
BAF	ab129184	aa 1-45	YES	YES (by abcam)
BAF-L	Sigma HPA042635	aa 12-252 of human BANF2	YES	YES
LBR	ab32535	aa 1-60*	YES	YES (by abcam)
GRP94	ab210960	aa 655-798	YES	YES (by abcam)
SPACA1	Sigma HPA026744	aa 93-153	YES (by Sigma)	YES (by Sigma)
Flag	Sigma F1804	DYKDDDDK	YES	YES
c-Myc	Sc-40	408-439 amino acids within C-domain of c-Myc	YES	YES
\square Tubulin	ab15246	426-ALEKDYEEVGVDSEGEEGEEY-450	NO	YES
Secondary:GAR	Invitrogen A11008	Goat Anti Rabbit - Alexa Fluor@488	*YES	-
Secondary:GAM	Invitrogen A11001	Goat Anti Mouse - Alexa Fluor@488	*YES	-
Secondary:GAM	Invitrogen A21121	Goat Anti Mouse - Alexa Fluor@488	*YES	-
Secondary:GAM	Invitrogen A11003	Goat Anti Mouse - Alexa Fluor@546	*YES	-
Secondary:DAR	Invitrogen A31573	Donkey Anti Rabbit – Alexa fluor@647	*YES	-

Table S2: Antibodies used in immunofluorescence and western blot analyses. For primary antibodies, IF and Western tests refer to affinity tests by transfection into tissue culture cells (Figure S1). For secondary antibodies, this refers to the absence of IF signal when antibody is used without a primary antibody.